Science of the Total Environment 957 (2024) 177290

Contents lists available at ScienceDirect

Science of the Total Environment

journal homepage: www.elsevier.com/locate/scitotenv

Controls on spatial variation in porewater methane concentrations across United States tidal wetlands

Erika L. Koontz [a,ab,*], Sarah M. Parker [a], Alice E. Stearns [a], Brian J. Roberts [b], Caitlin M. Young [b], Lisamarie Windham-Myers [c], Patricia Y. Oikawa [d], J. Patrick Megonigal [a], Genevieve L. Noyce [a], Edward J. Buskey [e], R. Kyle Derby [f], Robert P. Dunn [g], Matthew C. Ferner [h], Julie L. Krask [g], Christina M. Marconi [e], Kelley B. Savage [e], Julie Shahan [d], Amanda C. Spivak [i], Kari A. St. Laurent [j], Jacob M. Argueta [k], Steven J. Baird [k], Kathryn M. Beheshti [l], Laura C. Crane [m], Kimberly A. Cressman [n], Jeffrey A. Crooks [o], Sarah H. Fernald [q], Jason A. Garwood [p], Jason S. Goldstein [m], Thomas M. Grothues [r], Andrea Habeck [r], Scott B. Lerberg [s], Samantha B. Lucas [p], Pamela Marcum [aa], Christopher R. Peter [t], Scott W. Phipps [u], Kenneth B. Raposa [v], Andre S. Rovai [w,x], Shon S. Schooler [y], Robert R. Twilley [w], Megan C. Tyrrell [z], Kellie A. Uyeda [o], Sophie H. Wulfing [b], Jacob T. Aman [m], Amanda Giacchetti [t], Shelby N. Cross-Johnson [f], James R. Holmquist [a,*]

[a] *Smithsonian Environmental Research Center, 647 Contees Wharf Road, Edgewater, MD 21037, United States of America*
[b] *Louisiana Universities Marine Consortium, 8124 Highway 56, Chauvin, LA 70344, United States of America*
[c] *California Delta Stewardship Council, 715 P Street, 15-300, Sacramento, CA 95814, United States of America*
[d] *California State University-East Bay, 25800 Carlos Bee Blvd, Hayward, CA 94542, United States of America*
[e] *University of Texas Marine Science Institute, 750 Channel View Drive, Port Aransas, TX 78373, United States of America*
[f] *Maryland Department of Natural Resources, 580 Taylor Avenue, Annapolis, MD 21401, United States of America*
[g] *North Inlet-Winyah Bay National Estuarine Research Reserve, Baruch Marine Field Laboratory, 2306 Crabhall Rd, Highway 17 N, Georgetown, SC 29440-1901, United States of America*
[h] *San Francisco Bay National Estuarine Research Reserve, San Francisco State University, 3150 Paradise Drive, Tiburon, CA 94920, United States of America*
[i] *University of Georgia, Marine Sciences Department, 325 Sanford Drive, Athens, GA 30602, United States of America*
[j] *Delaware Department of Natural Resources and Environmental Control, 818 Kitts Hummock Road, Dover, DE 19901, United States of America*
[k] *Kachemak Bay National Estuarine Research Reserve, 2181 Kachemak Drive, Homer, AK 99603, United States of America*
[l] *University of California, Santa Barbara, Marine Science Institute, Santa Barbara, CA 93106, United States of America*
[m] *Wells National Estuarine Research Reserve, 342 Laudholm Farm Road, Wells, ME 04090, United States of America*
[n] *Grand Bay National Estuarine Research Reserve, 6005 Bayou Heron Road, Moss Point, MS 39562, United States of America*
[o] *Tijuana River National Estuarine Research Reserve, 301 Caspian Way, Imperial Beach, CA 91932, United States of America*
[p] *Apalachicola National Estuarine Research Reserve, Florida Department of Environmental Protection, 108 Island Drive, Eastpoint, FL 32328, United States of America*
[q] *Hudson River National Estuarine Research Reserve, 256 Norrie Point Way, Staatsburg, NY 12580, United States of America*
[r] *Rutgers University Marine Field Station, 800 c/o 132 Great Bay Blvd, Tuckerton, NJ 08087, United States of America*
[s] *Chesapeake Bay National Estuarine Research Reserve in Virginia at the Virginia Institute of Marine Science, Gloucester Point, VA 23062, United States of America*
[t] *Great Bay National Estuarine Research Reserve, 89 Depot Road, Greenland, NH 03840, United States of America*
[u] *Weeks Bay National Estuarine Research Reserve, 11300 U. S. Highway 98, Fairhope, AL 36532, United States of America*
[v] *Narragansett Bay National Estuarine Research Reserve, PO Box 151, Prudence Island, RI 02872, United States of America*
[w] *Louisiana State University, Department of Oceanography and Coastal Sciences, Baton Rouge, LA 70803, United States of America*
[x] *U.S. Army Engineer Research and Development Center, Halls Ferry Rd., Vicksburg, MS 39180, United States of America*
[y] *South Slough National Estuarine Research Reserve, 61907 Seven Devils Rd., P.O. Box 5417, Charleston, OR 97420, United States of America*
[z] *Waquoit Bay National Estuarine Research Reserve, 131 Waquoit Highway, Waquoit, MA 02536, United States of America*
[aa] *Guana Tolomato Matanzas National Estuarine Research Reserve, 505 Guana River Rd #6527, Ponte Vedra Beach, FL 32082, United States of America*
[ab] *Horn Point Laboratory, University of Maryland Center for Environmental Science, 2020 Horns Point Road, Cambridge, MD 21613, United States of America*

* Co-corresponding authors.
E-mail addresses: ekoontz@umces.edu (E.L. Koontz), HolmquistJ@si.edu (J.R. Holmquist).

https://doi.org/10.1016/j.scitotenv.2024.177290
Received 21 August 2024; Received in revised form 26 October 2024; Accepted 27 October 2024
Available online 16 November 2024

HIGHLIGHTS

- Methane variance was highest along environmental gradients and between sites.
- Sulfate was negatively and non-linearly correlated with methane concentration.
- Salinity was a significant, but weaker proxy for methane concentration.

GRAPHICAL ABSTRACT

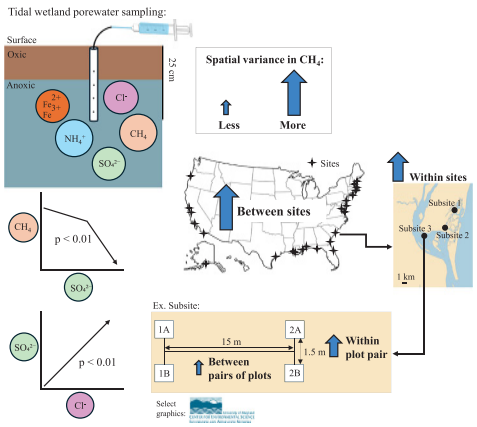

ARTICLE INFO

Editor: Jay Gan

Dataset link: Dataset: Porewater covariates from coastal tidal wetlands in the United States (Original data)

ABSTRACT

Tidal wetlands can be a substantial sink of greenhouse gases, which can be offset by variable methane (CH_4) emissions under certain environmental conditions and anthropogenic interventions. Land managers and policymakers need maps of tidal wetland CH_4 properties to make restoration decisions and inventory greenhouse gases. However, there is a mismatch in spatial scale between point-based sampling of porewater CH_4 concentration and its predictors, and the coarser resolution mapping products used to upscale these data. We sampled porewater CH_4 concentrations, salinity, sulfate (SO_4^{2-}), ammonium (NH_4^+), and total Fe using a spatially stratified sampling at 27 tidal wetlands in the United States. We measured porewater CH_4 concentrations across four orders of magnitude (0.05 to 852.9 μM). The relative contribution of spatial scale to variance in CH_4 was highest between- and within-sites. Porewater CH_4 concentration was best explained by SO_4^{2-} concentration with segmented linear regression ($p < 0.01$, $R^2 = 0.54$) indicating lesser sensitivity of CH_4 to SO_4^{2-} below 0.62 mM SO_4^{2-}. Salinity was a significant proxy for CH_4 concentration, because it was highly correlated with SO_4^{2-} ($p < 0.01$, $R^2 = 0.909$). However, salinity was less predictive of CH_4 with segmented linear regression ($p < 0.01$, $R^2 = 0.319$) relative to SO_4^{2-}. Neither NH_4^+, total Fe, nor relative tidal elevation correlated significantly with porewater CH_4; however, NH_4^+ was positively and significantly correlated with SO_4^{2-} after detrending CH_4 for its relationship with SO_4^{2-} ($p < 0.01$, $R^2 = 0.194$). Future sampling should focus on within- and between-site environmental gradients to accurately map CH_4 variation. Mapping salinity at sub-watershed scales has some potential for mapping SO_4^{2-}, and by proxy, constraining spatial variation in porewater CH_4 concentrations. Additional work is needed to explain site-level deviations from the salinity-sulfate relationship and elucidate other predictors of methanogenesis. This work demonstrates a unique approach to remote team science and the potential to strengthen collaborative research networks.

1. Introduction

Tidal wetlands are increasingly recognized for their contributions to the global methane (CH_4) budget emitting 0.76 Tg CH_4 $year^{-1}$ (Rosentreter et al., 2023), which offsets a portion of the carbon dioxide (CO_2) they sequester. Human activities have perturbed both CH_4 emissions (Kroeger et al., 2017) and carbon sequestration (Pendleton et al., 2012; Tan et al., 2020) and therefore have the potential to contribute to natural climate solutions that improve carbon removal and reduce greenhouse gas (GHG) emissions with appropriate management actions (Chmura et al., 2003; Mcleod et al., 2011; Fargione et al., 2018; Arias-Ortiz et al., 2021). Quantifying CH_4 emissions from tidal wetlands is vital due to the impact of CH_4 on radiative forcing in the atmosphere which is 45× that of CO_2 over 100 years from sustained sources of CH_4 (refer to Supplemental Table 1 in Neubauer and Megonigal 2015). However, significant uncertainties remain with spatial variation among tidal wetlands in the production and emission of CH_4 at regional and global scales (Xiao et al., 2024). New ground data and more detailed maps of wetland subclasses are needed for improving coastal GHG inventorying at a national scale (Holmquist et al., 2018), and for improving the classification of sector-based CH_4 emissions (Nesser et al., 2024). Wider-scale monitoring of CH_4 fluxes will require intensive field-based sampling with specialized equipment to effectively capture spatial variability (Needelman et al., 2018; Derby et al., 2022).

Understanding spatial scaling is a vital part of strategically deploying ground-based monitoring (Johnson et al., 2007), integrating ground and remote sensing data (Guo et al., 2017), and evaluating biogeochemical relationships at policy-relevant scales (Corstanje et al., 2008a, 2008b). Methane production is influenced by many processes that operate at different spatial scales of aggregation. For example, at the scale of individual soil particles, methanogenesis is spatially heterogeneous due to the presence of anoxic (Keiluweit et al., 2018) or oxic (Määttä and Malhotra, 2024) microsites. At the scale of meters, methanogenesis is spatially variable due to microtopography and variability in the depth of the water table (Perryman et al., 2022). Within watersheds, methanogenesis varies due to estuary-wide gradients in salinity and elevation (Arias-Ortiz et al., 2024). Across continental-scale gradients, methanogenesis varies due to climate variables such as mean annual temperature (Arias-Ortiz et al., 2024) and perhaps geomorphic controls (Kirwan et al., 2023; Cotovicz Jr et al., 2024). Importantly, spatial scaling is distinct from sampling uncertainty, which affects individual measurements.

In tidal wetlands, CH_4 emissions are a result of the production of CH_4 in soils, fluxes from soil to surface through plants, diffusion or ebullition across the soil surface, and consumption of CH_4 by methanotrophs (Bubier et al., 1995; Couwenberg et al., 2011; Sutton-Grier and Megonigal 2011; Mueller et al., 2016; Santos et al., 2019; Bansal et al., 2020; Vroom et al., 2022; Bastviken et al., 2023). Methanogenesis can occur under oxic or anoxic conditions, with the former deviating from the dogma that CH_4 production is restricted to anoxic sediments (Perez-Coronel and Beman, 2022). In anoxic conditions, the presence of alternative terminal electron acceptors may substantially limit methanogenesis (Megonigal et al., 2004) or promote CH_4 oxidation. Microbial competition for organic carbon (electron donors) can inhibit methanogenesis in the presence of higher energy-yielding electron acceptors such as SO_4^{2-} (Winfrey and Zeikus, 1977; Mountfort et al., 1980; Lovley and Klug, 1983; Kristjansson and Schönheit, 1983). Sulfate is a substrate for anaerobic CH_4 oxidation as a second mechanism for inhibiting the accumulation of CH_4 in porewater and emission of CH_4 (Hinrichs and Boetius, 2002; Segarra et al., 2015). Such interactions between SO_4^{2-} availability and CH_4 cycling give rise to strong correlations between these compounds. For example, Keller et al. (2009) offered evidence for a segmented regression relationship between porewater CH_4 and SO_4^{2-}, where CH_4 concentration rapidly decreases above 4 mM SO_4^{2-} concentration. Importantly, while SO_4^{2-} reduction clearly suppresses methane emissions, the two processes nonetheless co-occur in tidal wetlands due to spatial separation in the soil profile, microsite heterogeneity, and the presence of methanogenic pathways that do not compete with SO_4^{2-} reducers.

In previous studies, salinity was used as a proxy for sulfate's role in inhibiting methane emissions, where SO_4^{2-} leads to sulfate-reducing bacteria outcompeting CH_4 producers (Winfrey and Zeikus, 1977; Mountfort et al., 1980; Lovley and Klug, 1983; Kristjansson and Schönheit, 1983). A literature review by Poffenbarger et al. (2011) found that porewater CH_4 decreased as salinity increased across a narrow range (0–6.8 psu). Many other studies support the well-established paradigm that SO_4^{2-} associated with salinity effectively suppresses CH_4 production in tidal wetlands (Chambers et al., 2013; Neubauer, 2013; Helton et al., 2014; Weston et al., 2014; Wilson et al., 2015; Wang et al., 2017). Keller et al. (2009) provided a singular dataset to relate salinity and SO_4^{2-}, but considerable variability in that dataset prevents robust interpretation of a relationship. Al-Haj and Fulweiler (2020) emphasized that co-located measurements of CH_4, salinity, and other relevant covariates are necessary to validate and understand scale-driven changes in drivers of CH_4 production across broader salinity gradients and geographical areas. Evidence for relationships between porewater CH_4 concentration and covariates exist in the literature, but limited data, indirect measurements of covariates, differences in methods, and contrasting conclusions yield uncertainty of these relationships in tidal wetlands.

Other variables such as water level, watershed nutrient status, and the presence of other terminal electron acceptors have the potential to influence methanogenesis as well. Due to their inherent tidal components, these wetland ecosystems experience diurnal or semidiurnal changes in water levels. The tidal cycle affects water table depth (Vann and Megonigal 2003), frequency (Tong et al., 2020) and duration of inundation (Bansal et al., 2020), which together contribute to temporal and spatial heterogeneity in oxic and anoxic conditions for CH_4 production. Tides also contribute additional heterogeneity in CH_4 production and emissions through variance in covariate supply. The land use surrounding the wetland may also impact the supply of nitrogen to the wetland (Bowen et al., 2020). Nitrate (NO_{3-}) can serve as an alternate terminal electron acceptor in anoxic conditions, promoting decomposition. Ammonium may influence the production of CH_4 by increasing plant productivity (Langley et al., 2013). Other porewater constituents such as ferric iron (Fe^{3+}) can act as alternative terminal electron acceptors as well (Zou et al., 2018).

Understanding which physical factors influence covariate concentrations and how these may explain observed variability in porewater CH_4 concentrations in wetlands is complex. Most previous research efforts have focused on either individual sites (Bartlett et al., 1987; Keller et al., 2009), or synthesizing disparate studies with different methodologies (Poffenbarger et al., 2011; Al-Haj and Fulweiler, 2020; Arias-Ortiz et al., 2024). Relationships have not been quantitatively validated across landscape-level spatial scales with a consistent methodology. Deployment of a lower cost, spatially broad coverage sampling design based on a participatory science framework (Bell et al., 2013; Hadj-Hammou et al., 2017) has the potential to assess the spatial scaling of methanogenesis in tidal wetlands to inform large monitoring investments as well as validate previously determined dominant driver and proxy relationships across wider spatial scales.

This study uses a USA-wide survey of porewater CH_4 concentration and associated covariates based on a stratified sampling plan. We focused on porewater CH_4 concentration instead of CH_4 fluxes for two reasons. First, concentration measurements are less intensive to sample when compared to fluxes in terms of work-hours and specialized equipment (Arias-Ortiz et al., 2021), making them more feasible within continental-scale survey contexts. Second, the presence of dissolved porewater CH_4 is an important antecedent condition to CH_4 emissions (Keller et al., 2009; Duan et al., 2023) and has been shown to be positively correlated with CH_4 emissions in wetlands (Yang et al., 2019; Villa et al., 2020; Capooci et al., 2024).We aimed to quantify relationships between porewater CH_4 variance at different spatial scales and validate previously reported relationships between CH_4 and its predictors along broader ranges of covariate concentrations. We tested the following hypotheses: (i) SO_4^{2-} is negatively correlated with CH_4 concentration, (ii) salinity is a proxy for SO_4^{2-} in predicting porewater CH_4 concentrations, and (iii) relative tidal elevation, total Fe, and NH_4^+ are secondary predictors of porewater CH_4 concentration.

2. Methods

2.1. Site descriptions and experimental design

Between 2020 and 2021, we sampled a total of 27 tidal wetland sites (20 of which were located in the National Estuarine Research Reserve System [NERRS]) across the conterminous United States and Alaska (Supplemental Table 1; Fig. 1A). Sampling was constrained to coastal emergent intertidal marshes, excluding swamps, tidal freshwater forested wetlands, mangroves, and lakes. Field sampling was completed from July to early December in 2020 and 2021 coinciding with each site's peak aboveground biomass season. To assess the regional and local scale of variability of porewater conditions, each site was sampled at 3 to 4 locations ('subsites', Fig. 1B). Porewater samples were collected at 4 plots within each subsite (Fig. 1C). Subsites were selected by site experts in order to maximize a dominant environmental gradient such as salinity, management, elevation, and/or inundation, and to maximize distance from each other.

At each subsite, four 0.25 m^2 areas ('plots') were sampled, for a total of 367 plots. Using a rolling tape measure, the first plot was located 20 m inland from the wetlands/creek edge. A visual marker was thrown behind the researcher to randomize the location of the first plot and eliminate observer bias. Plots were spatially stratified with 1.5 m separating a pair of plots and a second pair located 15 m apart (Fig. 1C). Orientation between the 15 m stratified pairs was selected from a randomized list of compass bearings (Corstanje et al., 2008a; Corstanje et al., 2008b). If any plot was located in a water feature or was otherwise inaccessible, another direction was selected.

2.2. Porewater sampling and analyses

Porewater samples were collected 10–25 cm subsurface using sipper wells or rhizon MOM samplers (Rhizosphere Research Products, Wageningen, Netherlands). The latter depth range was chosen to avoid

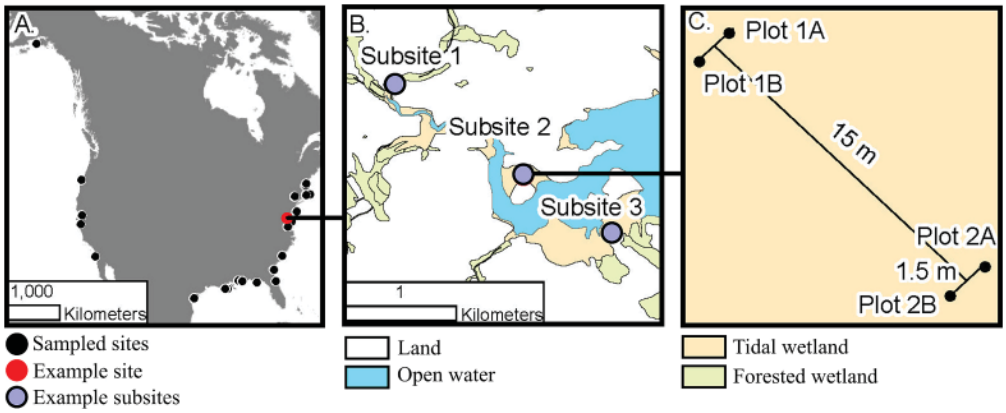

Fig. 1. A three-paneled figure illustrating this study's spatial scales of sampling. A.: An outline map of North America with all sampled sites; B.: example site (red circle from panel A.) with three example subsite locations, and; C.: a detailed view of example subsite 2 from panel B., demonstrating the paired plot-based sampling structure. Colors in panels B. and C.: beige (tidal wetland), green (forested wetland), white (land), blue (open water).

surface water entrapment (Zimmerman et al., 2005) and to ensure sufficient collection of porewater sample for an initial flushing (~20–30 mL) of the re-used sippers and for all analyses (up to 60 mL). The majority (90 %) of samples were collected using sippers that consisted of two sections: Tygon Masterflex tubing and Teflon PTFE chemical resistant tubing perforated with 3/32″ diameter holes and sealable aboveground with a stopcock (Noyce and Megonigal 2021). Within each plot, one porewater sampler was temporarily installed in a hole of the same diameter opened using a solid plastic rod. If little or no water was drawn from the initial sipper location, the sipper was re-located within the plot, and up to five attempts were made. If these attempts failed, the plot was moved and re-sampled. The stopcock on the sipper remained closed unless the sample was actively being withdrawn. Up to 90 mL of porewater was extracted from each well. Sippers and syringes were emptied, but not cleaned, and reused between plots. Single-use rhizon samples were collected for upwards of 2 h via vacuum pressure created in a syringe with a stopcock, held open with a retainer.

Porewater was extracted and filtered to 0.45 μm via a syringe-mounted filter (polyvinylidene fluoride) into 22 mL scintillation vials in order of priority: CH_4, SO_4^{2-}, Cl^-, NH_4^+, and total Fe. Dissolved CH_4 was extracted from an unfiltered sample of 12 mL porewater equilibrated with an equivalent volume of atmosphere within a syringe and shaken vigorously for 2 min (Megonigal and Schlesinger, 2002). The air sample was injected into a nitrogen (N_2) flushed 12 mL Labco (Lampeter, Wales, UK) exetainer via a single use needle attached to a filter to absorb excess water. The SO_4^{2-} and Cl^- samples were collected using 10 mL of porewater filtered into a scintillation vial containing approximately 1 mL of 5 % zinc acetate and sodium hydroxide buffer, and shaken to mix (Keller et al., 2009; Environmental Protection Agency, 1996). Up to 40 additional mL of porewater was collected and filtered into two vials to be analyzed for NH_4^+ and total Fe, respectively.

Methane samples were stored at air temperature (Faust and Liebig, 2018), while all other samples were kept on ice during collection and later frozen. Samples were shipped overnight on ice to the Smithsonian Environmental Research Center (Edgewater, MD, USA) and stored in a −20 °C freezer until analysis. Methane was measured on a Bruker Varian 450 gas chromatograph. Porewater CH_4 concentrations were derived from the slope of the line of known standard values, ranging from 100 to 100,000 ppm CH_4, and log-transformed to account for non-negative values.

Sulfate and Cl^- were analyzed on a Thermo Fisher (Waltham, MA, USA) Dionex Integrion (2019) following similar methods from Noyce and Megonigal (2021), where samples were separated using an A11 4 μm fast column using 32 mM of KOH as the eluent. The detection limit for SO_4^{2-} and Cl^- was calculated by multiplying the standard deviation of the lowest standard by three, respectively. Ammonium was used as an indicator of nutrient status and total Fe as an indicator of the potential for Fe^{3+} presence. Ammonium was analyzed using the Berthelot-salicylate colorimetric technique (Noyce et al., 2019). Total iron ($Fe^{2+} + Fe^{3+}$) concentrations were determined by the ferrozine method (Loeppert and Inskeep, 1996; Viollier et al., 2000) on a Shimadzu UV-1800 UV spectrophotometer and measured at the Louisiana Universities Marine Consortium.

2.3. Aboveground biomass assessment and longitude, latitude, and elevation data

The relative abundance and percent cover of each plant species was described in each plot using the Braun-Blanquet (1932) scale. A destructive harvest of 10 × 10 cm or 25 × 25 cm was conducted, clipping all stems within 2 cm of the marsh surface. Live stems were sorted by species, if possible. Aboveground necromass was pooled and not identified by species. All plant samples were dried at 60 °C until stable weight was reached (≥5 days), and then weighed with a Sartorius 1574A (Sartorius AG, Goettingen, Germany) or Ohaus STX 422 (Ohaus Corporation, Parsippany, New Jersey, U.S.) balance, to the microgram. The latitude, longitude, and elevation (NAVD88 vertical datum) of each plot was measured, if possible, using a cell-phone, Google Earth, hand-held Garmin (models: 73, Etrex 20×, GPSMap 64st or 78sc, Montana 600), SP80 RTK, Bad Elf GNSS, Trimble (Geo7x, R8s, R10, R12, R12i), Leica Sprinter 150 m or 250 m Digital Level, or Emlid Reach RS2.

2.4. Data analysis

Data visualization and multiple regression approaches were conducted in R (version 4.1.3, R Core Team, 2022). Additional figures were created using ArcGIS (version 10.8, Environmental Systems Research Institute, Inc., 2020). A Spearman's rank correlation was used to assess the relationship between the porewater covariates, aboveground biomass, and species richness. Data normality was tested using the Shapiro-Wilks normality test and visualized in histograms (Supplementary Fig. 1).

In order to quantify the relationship between spatial scale and porewater CH_4 variability, we partitioned variance attributable to each level of spatial hierarchy using a Bayesian random effects model (Hobbs and Hooten, 2015). We estimated the amount of variance present at each spatial scale using Eq. (1). Methane data were natural log-transformed.

$$ln(CH_4) = ln(\mu) + \beta_{1.5m,i} + \beta_{15m,j} + \beta_{within.site,k} + \beta_{between.site,l} \quad (1)$$

$$ln(\mu) \sim N(0, 1000)$$

$$\beta_{1.5m,i} \sim N(0, \sigma^2_{1.5m})$$

$$\beta_{15m,j} \sim N(0, \sigma^2_{15m})$$

$$\beta_{within.site,k} \sim N(0, \sigma^2_{within.site})$$

$$\beta_{between.site,l} \sim N(0, \sigma^2_{between.site})$$

$$\overline{1/\sigma^2} \sim \text{gamma}(0.001, 0.001)$$

where $CH_{4,i}$ is the methane concentration of datapoint i, μ is the mean CH_4 concentration, and each β is a random effect representing i individual plots (1.5 m), j 15 m-stratified plot pairs (15 m), k subsites (within-site), and l sites (between-site). Priors were uninformed with the prior for $\log(\mu)$ distributed as normal with a mean of zero and a variance of 1000 (Hobbs and Hooten, 2015). Each random effect was distributed as normal with a mean of zero and a variance attributed to that spatial level. Each spatial variance was assigned an inverse gamma prior with both alpha and beta parameters set to 0.001.

The model was fit in *rjags* using 4 chains and 5000 iterations (Plummer et al., 2021). Traceplots were examined to ensure model convergence on a single solution. Data were summarized as both the variance partitioned at each spatial level and the cumulative summed variance across each level (Corstanje et al., 2008a; Corstanje et al., 2008b). Data are presented as a percentage of total cumulative variance, with the mean estimate and standard error extracted from the posterior distributions of the parameters (Fig. 3).

We calculated relationships between CH_4 and porewater covariates SO_4^{2-}, NH_4^+, and total Fe, as well as between SO_4^{2-} and salinity using linear models. During initial data visualization we observed a breakpoint in the relationship between SO_4^{2-} and CH_4 and utilized a segmented regression (Muggeo, 2008). We compared the performance relative to parsimony of segmented regressions to single slope linear models using Akaike's Information Criteria.

We tested for potential secondary relationships with other predictors. To do this, we first detrended CH_4 for its relationship with SO_4^{2-} by calculating residuals as the difference between measured CH_4 and predicted CH_4 from its segmented regression relationship with sulfate concentration. We regressed the residuals against porewater NH_4^+, total

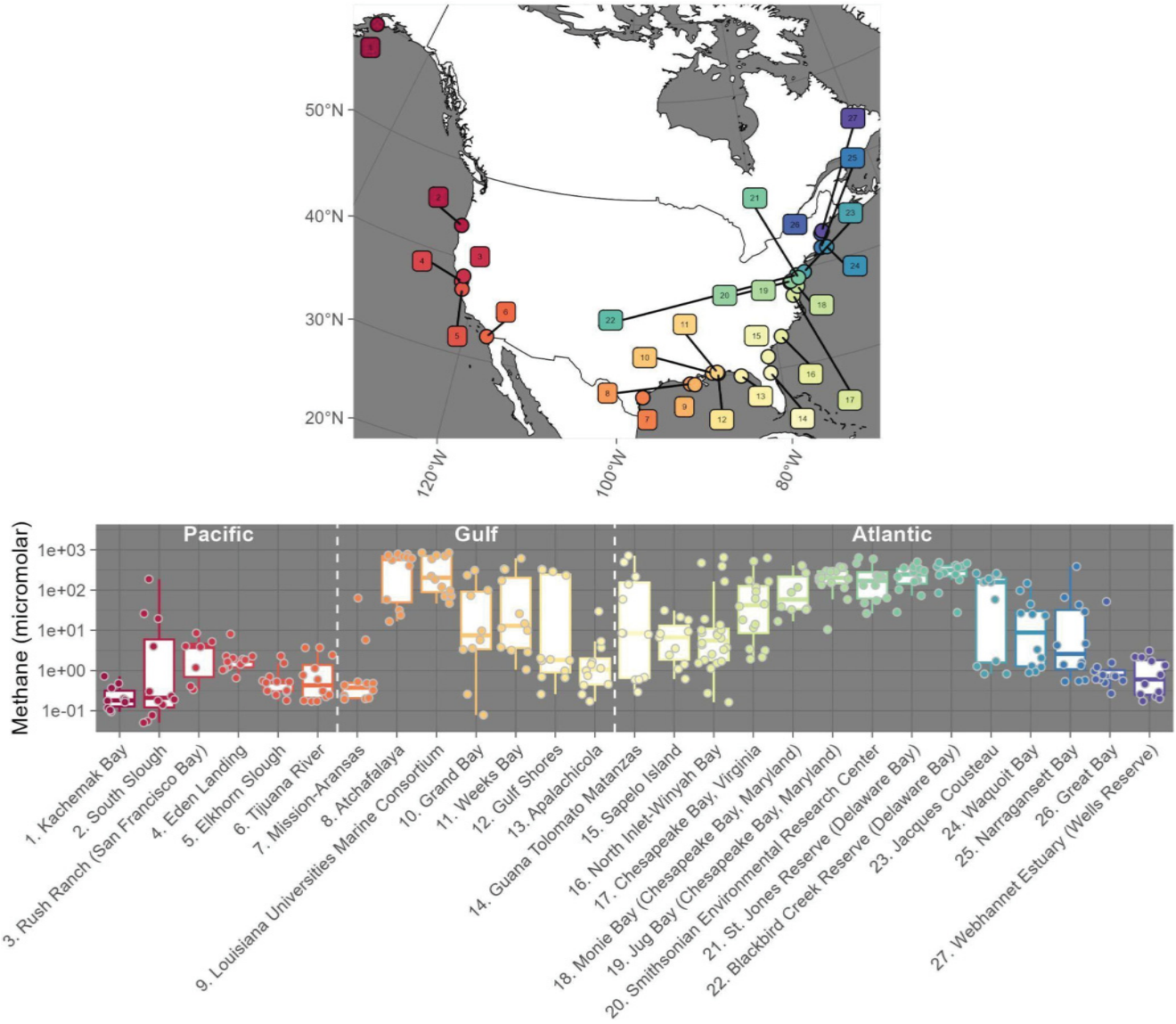

Fig. 2. Upper panel: a map of the U.S. with sites sampled (multi-colored dots) and numerically labeled 1–27 (moving counterclockwise from Alaska). Lower panel: log scale CH_4 box plots grouped by coast (Pacific, Gulf, Atlantic), labeled with site name and reference number. NERRS with multiple components that were sampled in separate years are labeled with the component name listed first, and followed by the NERR site name (ex. 18. Monie Bay [Chesapeake Bay, Maryland]).

Fe, and marsh platform elevation. To analyze the relationship between wetland elevation and residual variance in CH_4, we normalized elevation measured at the plots to tidal amplitude at mean high water (Z^*_{MHW}) referenced to the NAVD88 datum (Holmquist and Windham-Myers, 2022). Mean high water (MHW) and mean sea level (MSL) values were interpolated between NOAA (tidesandcurrents.noaa.gov) and Coastwide Reference Monitoring System (CRMS, lacoast.gov/crms/Home.aspx) tide gauges using ordinary kriging. For Kachemak Bay, Alaska, USA datums from the nearest complete NOAA tide gauge (Niksiki, AK, USA: 9455760) were used directly, rather than leveraging the kriging model fit across the distant regions of the contiguous United States.

3. Results

3.1. Dataset description

A total of 27 unique sites and 367 plots distributed across 19 coastal states were sampled (Fig. 2). Only 1 plot lacked Cl^- data and 2 plots lacked SO_4^{2-} data as they were below the detection limits of 1.503×10^{-4} Cl^- psu and 1.115×10^{-3} mM SO_4^{2-}, respectively. Porewater SO_4^{2-} measured from plots varied from below the detection limit to a maximum of 47.45 mM (Table 1, Supplemental Fig. 3). Due to limited porewater, 3 plots lacked a total Fe measurement and 5 lacked NH_4^+. Elevation data were collected at 156 plots, representing 13 sites. The dataset of sampled plots represents all salinity classes from fresh to brine (0.5–55 psu). Across all sites, 109 unique plant species were identified. Of those, 103 and 90 were identified to genus and species level, respectively (Supplemental Table 1).

3.2. Spatial variability of porewater methane concentration

The concentrations of porewater CH_4 samples (n = 332) used in analysis ranged from 0.05 to 852.9 μM, with a mean ± s.e. of 108 ± 0.56 μM (Table 1). Methane samples were collected from all plots (n = 367); however, some values were excluded due to sampling issues associated with rhizons, values below the detection limit, and samples collected from outlier habitat types (e.g. submersed vegetation beds) that were not targeted by this study. Including some omitted samples, CH_4 concentrations (n = 344) ranged from 0.05 μM to 7828 μM, with a mean ± s.e. of 163 ± 1.57 μM. Porewater CH_4 was increasingly variable at larger spatial scales (Fig. 3). Finer spatial scales contributed relatively less variance than coarser ones. The 1.5 m and 15 m spatial scales contributed (mean ± s.e.) 9.6 ± 2.2 % and 5.7 ± 2.2 % of the cumulative spatial variance, respectively. Within-site gradients and between-site differences accounted for 29.5 ± 7.9 % and 55.3 ± 9.6 % of the cumulative spatial variance, respectively.

Table 1
Minimum, maximum, and mean values for measured porewater covariates for all plots and by coast (Atlantic, Gulf, and Pacific).

Value	Minimum	Maximum	Mean
Covariate: CH_4 (μM)			
All plots	0.05	852.9	108
Atlantic	0.163	714.6	119.4
Gulf	0.078	852.9	163.9
Pacific	0.05	186.8	4.78
Covariate: Cl^- (ppt)			
All plots	0.021	55.22	17.28
Atlantic	0.021	42.52	14.02
Gulf	0.052	55.22	15.38
Pacific	3.824	53.4	28.94
Covariate: SO_4^{2-} (mM)			
All plots	<0.001*	47.45	10.57
Atlantic	<0.001*	31.5	7.495
Gulf	0.005	42.3	8.552
Pacific	2.463	47.45	21.85
Covariate: NH_4^+ (μM)			
All plots	33.04	641	103.7
Atlantic	33.04	641	83.41
Gulf	33.08	618.4	119.8
Pacific	34.88	459.4	141
Covariate: total Fe (μM)			
All plots	0.012	2966	54.32
Atlantic	0.015	2966	73.82
Gulf	0.016	618.2	47.63
Pacific	0.012	201.1	7.149

* Indicates that lowest value was below the instrument detection limit.

3.3. Correlations between porewater methane, sulfate, and salinity concentrations

Porewater CH_4 was negatively and significantly correlated with porewater SO_4^{2-} across the dataset ($\rho = -0.732$, $p < 0.01$; Supplemental Fig. 1). A segmented linear regression had higher explanatory power for the CH_4 and SO_4^{2-} relationship (both covariates log-transformed) over a single linear regression (Fig. 4A, Table 2). Furthermore, the segmented regression was statistically significant ($p < 0.01$) and resulted in a lower corrected Akaike Information Criterion (AICc) score (Table 2). The CH_4 and SO_4^{2-} resulted in a negative slope with a breakpoint of 0.62 mM SO_4^{2-} (Fig. 4A), characterized by a relatively flatter slope at concentrations lower than 0.62 mM SO_4^{2-}, and steeper slopes at concentrations >0.62 mM SO_4^{2-} (Fig. 4A, Eq. 2). Fifty-nine data points informed the slope below the breakpoint, and 306 data points informed the slope above the breakpoint, described in Eq. 2:

$$ln(CH_4) = \begin{cases} 4.934 - 0.0615 * ln(SO_4^{2-}); \text{if } ln(SO_4^{2-}) \le -0.478 \\ 4.963 - 1.358(ln[SO_4^{2-}] + 0.478); \text{if } ln(SO_4^{2-}) > -0.478 \end{cases} \quad (2)$$

where CH_4 concentration is in micromolar (μM) and SO_4^{2-} is in millimolar (mM).

The Spearman's rank correlation also indicated that salinity and SO_4^{2-} were the most strongly positive correlated variables ($\rho = 0.935$, $p < 0.001$; Fig. 4B and Supplemental Fig. 1). A single linear regression that modeled salinity and SO_4^{2-} was positive, significant, and had strong explanatory power (Table 2). While the relationship between salinity and SO_4^{2-} is significant and positively linear, this linearity is only clearly observed at salinities >8 psu and $SO_4^{2-} > 1$ mM (Fig. 4B, Eq. 3). The area of these values, and thus the change in relationship from weakly to strongly linear, is indicated by the pair of horizontal and vertical dashed lines in panel B (Fig. 4). Below these values, the linearity of the relationship weakens as the spread between data points increases.

$$SO_4^{2-} = -2.969 + 0.789S \quad (3)$$

where S is salinity (psu) and SO_4^{2-} is sulfate concentration in millimolar (mM).

Porewater CH_4 and salinity were also significantly and inversely correlated ($\rho = -0.576$, $p < 0.001$; Fig. 4C and Supplemental Fig. 1). Due to the strong linear relationship between salinity and SO_4^{2-} as well as the relationship between CH_4 and salinity (Fig. 4C), we expected that salinity may have similar predictive power for porewater CH_4 (Eq. 4). However, substituting salinity for SO_4^{2-} concentration results in a relationship with lower predictive ability than SO_4^{2-} on its own (Fig. 4C). A simple linear model produces a significant, negative relationship, but the segmented linear regression provides more predictive accuracy (Table 2):

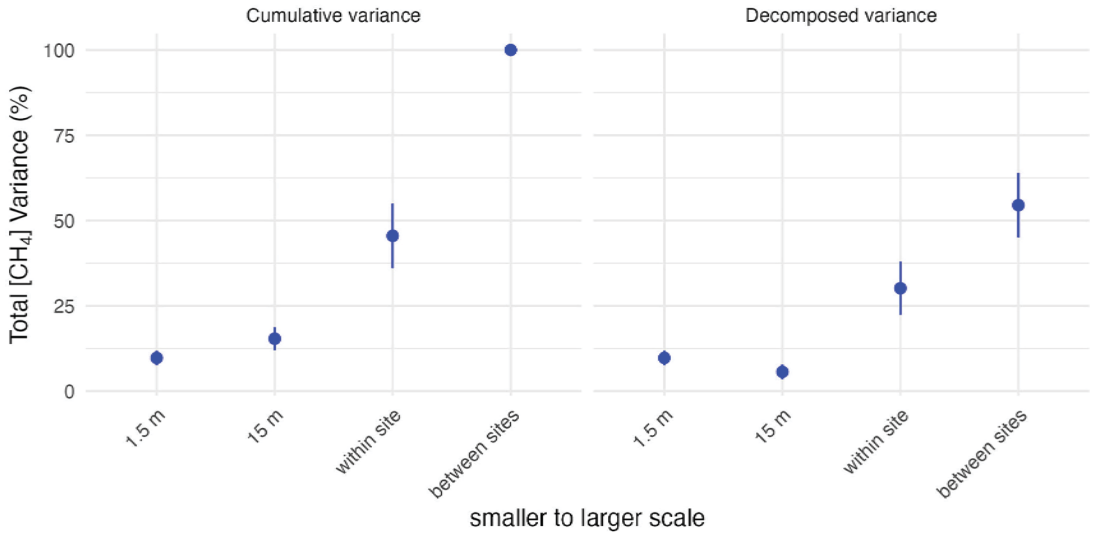

Fig. 3. Variance in log-transformed porewater CH_4, expressed as a percentage of total variance, at four spatial scales ordered from left to right, smallest to largest scale: 1.5 m (m), 15 m, within site [along site-specific gradients], and between-sites. Points represent mean estimates and segments represent the standard error of the estimate. Spatial variance is presented both as cumulative variance, with variability propagated from smaller to larger scales, as well as decomposed variance, variability attributable to each spatial level.

$$ln(CH_4) = \begin{cases} 3.795 - 0.210^{*}ln(S); \text{if } ln(S) \leq 2.445 \\ 3.282 - 2.840(ln[S] - 2.445); \text{if } ln(S) > 2.445 \end{cases} \quad (4)$$

Both porewater SO_4^{2-} and salinity correlated strongly with porewater CH_4, but the modeled relationship between SO_4^{2-} and CH_4 explains more variability in CH_4 (Eq. 2, Table 2). Additional relationships between CH_4 and other covariates were investigated to explain remaining variability in CH_4. Since some variability in CH_4 was explained by SO_4^{2-}, we detrended the CH_4 residuals, therefore removing the explanatory effect of SO_4^{2-} on the CH_4 residuals. Following that, we investigated the remaining variability found in the CH_4 residuals (Eq. 2) by regressing them separately against log-transformed NH_4^+, total Fe, and Z^*_{MHW}, the latter which is a proxy for tidal inundation. We detected a significant, positive correlation between CH_4 residuals and NH_4^+ (Table 2). A simple linear model was significant and positive, but with lower explanatory power than a segmented regression with a breakpoint at 44 μM NH_4^+ (Fig. 4D). Significant correlations were not detected between detrended CH_4 residuals and total Fe ($p = 0.80$) nor Z^*_{MHW} ($p = 0.27$).

4. Discussion

Our national-scale study of tidal wetland CH_4 concentration produced a unique and unprecedented spatially-nested dataset of co-located porewater measurements from tidal wetlands along all coastlines of the USA. We provide important information on spatial scaling properties of CH_4 concentration that are useful for remote sensing, inventorying, and planning new ground monitoring. We also tested three hypotheses regarding the predictability of CH_4 concentration over landscape scales. Our first hypothesis was supported as we observed a negative correlation between porewater concentrations of CH_4 and SO_4^{2-}, an energetically favorable terminal electron acceptor under anoxic conditions that is present in seawater. Our second hypothesis was supported; salinity was a significant, though comparatively weak, proxy for CH_4 concentration in the absence of direct SO_4^{2-} measurements. Our third hypothesis, that nutrient enrichment, the presence of Fe, and tidal elevation would be important secondary predictors was partially supported with NH_4^+ being weakly correlated with variance unexplained by the CH_4-SO_4^{2-} relationship.

In this section, we discuss how scaling and covariate relationships can inform future coastal wetland carbon monitoring. We compare the breakpoints in relationships between porewater CH_4 and its covariates to the results of previous studies. Finally, we suggest future research directions, and reflect on the strengths of a collaborative participatory-science approach.

4.1. Implications of spatial scaling and covariate relationships for monitoring

Our study considered the importance of spatial scaling on porewater CH_4 concentrations. Heterogeneity in porewater CH_4 was detected even at relatively fine spatial scales, but the proportion of variance was least at the smallest spatial scales. This result recalls Tobler's (1970, 2004) first law of geography, where increased proximity between measurements results in increased similarities between them. Statistics applies this principle via measures of spatial autocorrelation to assess spatial dependence between measurements (Crawford, 2009). We detected a sharp increase in variance when scaling along within-site gradients and between-sites. Within-site variation was attributed mostly to variation in salinity associated with SO_4^{2-}. The between-site variance increase may be explained by differences in dominant coastal typologies of the sites we sampled, their climate zones, or both (Dürr et al., 2011; Beck et al., 2018; Kirwan et al., 2023). Together, the key results supporting the importance of within-site, and between-site variability, and the dominance of SO_4^{2-} as a process-based predictor, can inform new monitoring plans for coastal CH_4 monitoring.

Our results inform future efforts to develop maps of CH_4-relevant processes in three ways. First we show that the scale of moderate-resolution remote sensing will be able to capture the majority of spatial variance in CH_4. Maps of surface water (Huang et al., 2018), vegetation (Adam et al., 2010), and salinity (Murphy et al., 2010) are typically made using 10–30 m spatial resolution imagery products (e.g., from Sentinel and Landsat satellites). According to our dataset, 85 % of the variance in CH_4 concentration occurs at scales >15 m and could be hypothetically detected by these remote sensing products. The remaining 15 % of variance occurs at sub-pixel resolution that would be averaged out by these mapping techniques. Second, this study reinforces the need for tidal wetland subtype maps which include intermediate salinity classes, or, more ideally, continuous salinity predictions (Holmquist et al., 2018). The dataset presented in this paper itself could potentially be used as calibration and validation data in the creation of such a map (Koontz et al., 2024). Third, information on spatial scaling could be used as priors in future efforts to explicitly fuse high-resolution

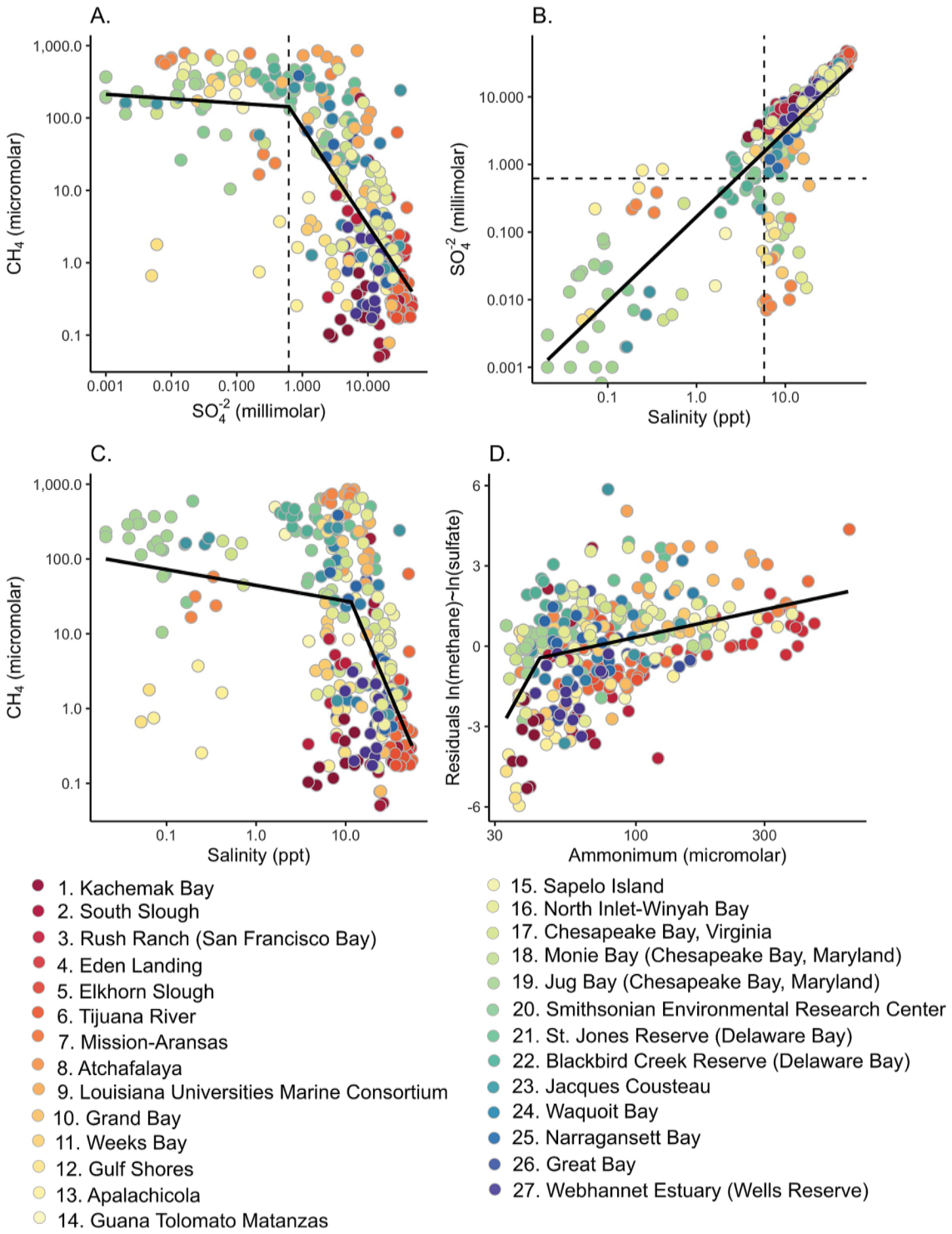

Fig. 4. Porewater covariate relationships in four panels: A. sulfate and methane (both log-transformed); B. salinity and sulfate; C. salinity and methane; and D. ammonium and residual variance in methane (log-transformed) after removing variance explained by the concentration of sulfate (log-transformed). Solid, black lines with a break (segmented linear regression) indicate that the relationship between covariates significantly changes within the range of measured concentrations. Dashed lines correspond to concentration break points where the relationship between covariates changes, and are discussed in text.

field data to moderate-resolution remote sensing using Bayesian hierarchical modeling (Guo et al., 2017), overcoming the issue of scale mismatch between ground and remotely sensed data.

For future monitoring of methanogenesis in tidal wetlands, our analysis supports sampling designs that focus first on prioritizing more sites across wide climate gradients and/or geomorphic classes, and second on capturing environmental variation within watersheds. Additional studies and carbon inventories could use this continental-scale dataset to generate informed sampling strategies that optimize information content of new data relative to the cost of deploying and maintaining monitoring infrastructure (Hurtt et al., 2022; Brown et al., 2023).

Our results suggest that to map CH_4 concentration, future research should focus on SO_4^{2-} because salinity is an imperfect proxy. While a

Table 2
Statistical outputs for the modeled relationships between porewater covariates. The *p*-value, R^2, and Akaike Information Criterion with standard correction (AICc) values are provided for two model types, single linear regression and segmented linear regression, if applicable.

Modeled relationship	CH_4 (μM) and SO_4^{2-} (mM)		
Value	*p*-Value	R^2	AICc
Single linear regression	<0.01	0.45	1401
Segmented linear regression	<0.01	0.54	1346

Modeled relationship	Salinity (ppt) and SO_4^{2-} (mM)		
Value	*p*-Value	R^2	AICc
Single linear regression	<0.01	0.909	N/A

Modeled relationship	CH_4 (μM) and Salinity (ppt)		
Value	*p*-Value	R^2	AICc
Single linear regression	$p < 0.01$	0.191	1544
Segmented linear regression		0.319	1489

Modeled relationship	CH_4 (μM) residuals (SO_4^{2-} effect removed) and NH_4^+ (μM)		
Value	*p*-Value	R^2	AICc
Single linear regression	<0.01	0.1663	1281
Segmented linear regression	<0.01	0.1942	1272

dominant predictor of CH_4, SO_4^{2-} is more rarely measured compared to the much more ubiquitous salinity measurements (Tong et al., 2010; Poffenbarger et al., 2011). Our results supported a high degree of correlation between SO_4^{2-} and salinity ($R^2 = 0.909$). However, the relationship between salinity and CH_4 had lower, though significant, explanatory power ($R^2 = 0.319$) compared to the direct SO_4^{2-} relationship ($R^2 = 0.54$). Part of this could be due to a decoupling of the strength of the salinity-SO_4^{2-} relationship at low salinities, particularly below 5 psu due to SO_4^{2-} depletion at low concentrations.

Although this study provided evidence that SO_4^{2-}, and by proxy salinity, explain a significant proportion of spatial variance in porewater CH_4 concentrations, other studies show that inundation and the presence of other terminal electron acceptors may still be important to future mapping and monitoring of CH_4 properties. Arias-Ortiz et al. (2024) showed that in a U.S. wide synthesis of CH_4 emissions, salinity class was the dominant predictor, but that inundation class and mean annual temperature are important secondary predictors. In pan-Arctic wetlands, spatial variability in CH_4 emissions is dominantly controlled by water table depth, as well as soil temperature, and vegetative functional types (Bao et al., 2021). In freshwater, nontidal and tropical wetlands with distinct dry and wet seasonality, inundation timing and duration are more important drivers for CH_4 emissions than SO_4^{2-} or salinity (Li et al., 2024). In our study, Z^*_{MHW}, a proxy for tidal inundation, was not a significant secondary predictor of CH_4. This may reflect high uncertainties in Z^*_{MHW} (Holmquist and Windham-Myers, 2022), weakness of Z^*_{MHW} as a proxy for inundation (Cassaway et al., 2024), or our study having too few elevation measurements to be representative of actual gradients.

In addition to water level, future mapping and monitoring efforts may want to more intensively investigate watershed-level land use effects on the availability of nutrients and alternative terminal electron acceptors. We used NH_4^+ as a proxy for nutrient status and found evidence indicating that organic nitrogen could interact with the CH_4-SO_4^{2-} relationship with the potential to cause watershed-specific anomalies in CH_4 concentration. In freshwater wetlands with or without tidal exchange, several other electron acceptors in addition to SO_4^{2-} catalyze CH_4 oxidation, including nitrite (NO_2^-) (Hu et al., 2014), and nitrate (Segarra et al., 2013). Reactive nitrogen concentration is typically low in tidal wetlands (Valiela and Teal, 1974), but can be elevated in nutrient rich agricultural runoff (Pardo et al., 2011). Finally, while our study found no relationship between total Fe and CH_4 concentrations, a previous study indicated that Fe can occur in elevated amounts in agricultural runoff (Zou et al., 2018), which provides a preferable terminal electron acceptor Fe^{3+} (Sivan et al., 2011) that can reduce methanogenesis when added to a wetland (Zou et al., 2018). Taken together, the role of agricultural runoff and nutrient enrichment on methanogenesis and CH_4 oxidation could potentially be an important aspect of future mapping and monitoring.

4.2. Novel relationships between sulfate, methane, and ammonium

We observed a previously undocumented significant change in the slope of the CH_4-SO_4^{2-} relationship defined by a breakpoint of 0.62 mM SO_4^{2-}, with high sensitivity to changing SO_4^{2-} below the breakpoint and low sensitivity above (Fig. 4A). This relationship presumably reflects the concentration at which SO_4^{2-} reduction rates become limited by SO_4^{2-} availability (Winfrey and Zeikus, 1977; Mountfort et al., 1980; Lovley and Klug, 1983; Kristjansson and Schönheit, 1983). Below our breakpoint of 0.62 mM SO_4^{2-}, we suggest that the ability of SO_4^{2-}-reducing bacteria to outcompete methanogens progressively weakens. However, only acetoclastic and hydrogenotrophic methanogens are likely to be positively impacted by reductions in SO_4^{2-}, whereas the activity of methylotrophic methanogens is unaffected by SO_4^{2-}-reducing bacteria (Seyfferth et al., 2020).

The CH_4-SO_4^{2-} relationship is distinct from previously reported breakpoints that were developed using much smaller sample sizes and observed within singular wetland sites (Bartlett et al., 1987; Keller et al., 2009; Poffenbarger et al., 2011). In studies of lacustrine and marine ecosystems, published breakpoints are at lower SO_4^{2-} concentrations, ranging between 0.008 and 0.04 mM SO_4^{2-} (Lovley and Klug, 1983; Ingvorsen et al., 1984; Kuivila et al., 1989; Sinke et al., 1992; Holmer and Storkholm, 2001). At the higher end, Poffenbarger et al. (2011) noted a breakpoint of 4 mM SO_4^{2} in tidal wetlands, over which CH_4 concentrations were negligible.

We also discovered a novel breakpoint and a significant relationship between NH_4^+ and CH_4 that explained additional variance in porewater CH_4 concentrations and provided some support for our third hypothesis. After detrending the effects of SO_4^{2-} on CH_4, NH_4^+ was positively and significantly correlated with CH_4, with a breakpoint at 44 μM NH_4^+ (Fig. 4D). Perhaps the most parsimonious explanation is that high NH_4^+ availability supports high plant production and soil carbon inputs that support methanogenesis (Langley et al., 2013), a process that is generally carbon-limited (Megonigal et al., 2004). Another potential explanation for this relationship could be that NH_4^+ inhibits CH_4 oxidation in wetlands when concentrations of NH_4-N are 30× that of CH_4, allowing CH_4 to persist in porewater (Van Der Nat et al., 1997; Laanbroek, 2010). We hypothesize that below 44 μM NH_4^+, CH_4 oxidation is primarily occurring, and above 44 μM NH_4^+, NH_4^+ oxidation inhibits CH_4 oxidation. Alternatively, this relationship may reflect the coupling of NO_3^- to anammox, of which NH_4^+ is a product, and NO_2^--dependent anaerobic CH_4 oxidation, leading to some CH_4 consumption (Zhu et al., 2010; Shen et al., 2015). Within tidal wetlands, the nitrogen species are determined, in part, by internal nitrogen cycling (Noyce and Megonigal 2021), exogenous supply from tidal waters (Krask et al., 2022), inundation duration (Chowdhury and Dick, 2013), and surrounding land uses (Weston et al., 2006). The mechanisms that underpin the NH_4 and CH_4 relationship are unclear but suggest that available reactive nitrogen species may partially determine the fate of porewater CH_4.

4.3. Potential limitations and caveats inherent in a kit-based sampling approach

The data from this highly collaborative kit-based sampling effort of U.S. tidal wetland porewaters is valuable to constrain spatial variation in porewater CH_4 and its covariates. However, we acknowledge some results are limited in their application and warrant caveats. Limitations and caveats arise from the fact that we focused on a spatially-rich, though temporally limited, sampling strategy, variability in site characteristics reduced our ability to sample heavy clays, and our need to focus on stable analytes limited some of the more detailed biogeochemical inferences that could be made.

First, in this study, we prioritized a spatially extensive deployment during each site's peak aboveground biomass season across a wide variety of sites that span the entire coastline of the USA, which did not permit a time series of measurements to occur. However, previous studies show that measurements of CH_4 emissions taken during peak aboveground biomass growing conditions tend to reliably scale to annual fluxes (Bridgham et al., 2006). Further, we cite the strong-relationship between CH_4 and SO_4^{2-} ($R^2 = 0.54$) as evidence that this relationship, at least during the peak aboveground biomass growing season, is likely robust across sites. We hypothesize that some of the residual variance (46 %) may be explained by time specific phenomena such as slight differences in the timing relative to seasonal cycles within sites or time since the last large tidal flood event. Previous studies have focused on datasets that maximized observations of the important temporal scales of CH_4 variability (Bartlett et al., 1987; Keller et al., 2009; Tong et al., 2010; Poffenbarger et al., 2011; Derby et al., 2022). This new dataset provides an important counterpart to these temporally rich analyses and future work should integrate the strengths of both approaches.

A second caveat is related to site characteristics and porewater sampling methodology. We collected porewater using "sippers" from the majority of our 367 sampling plots. However, this was not possible for 22 plots consisting of mineral dominated soils with high clay concentrations, for which we used rhizons (Shotbolt, 2010). Rhizon samples of porewater CH_4 yielded concentrations <6.23 μM, meaning that the rhizon sampling method likely underestimated the CH_4 concentration. We hypothesize that a small fraction of CH_4 was actually dissolved in the porewater, and the rest of the porewater CH_4 concentration was contained within poorly soluble CH_4 micro-bubbles that did not pass through the rhizon filter with a nominal pore size of 0.6 μM. As a result, rhizon measurements of porewater CH_4 were excluded from analysis, but the remaining covariates collected with rhizons remained in the dataset (Song et al., 2003; Seeberg-Elverfeldt et al., 2005; Chen et al., 2015). Future studies should be aware of this potential methodological limitation.

Although the kit-based sampling design enabled us to effectively capture spatial variation of porewater CH_4 concentration and assess covariates, the logistics of mail-in kits limited analysis to those analytes that could be easily stabilized. For example, we focused on the availability of terminal electron acceptors rather than electron donors such as dissolved organic carbon (DOC). We assumed that terminal electron acceptors would be rate limiting and therefore explain more variation. We also focused on total Fe rather than reactive Fe^{3+}, and NH_4^+ as a proxy for nutrient status rather than other reactive nitrogen species. Should future work overcome logistical constraints, we recommend measurements of additional electron acceptors that may increase understanding of spatial variability in porewater CH_4. We specifically recommend future studies to include measurements of porewater concentrations of NO_3^-, NO_2^-, manganese, and Fe^{3+} alongside the five covariates we measured.

4.4. Recommendations for future research

The results of this unprecedented, diverse, and large porewater dataset and its analysis uncovers new research priorities. First, the relationship between porewater CH_4 and CH_4 fluxes across spatial scales needs to be better understood. Second, more detailed microbial information on the presence of methanogens and methanotrophs is needed. We close by discussing the benefits of the participatory nature of this study, and using it as a template for future research.

While porewater CH_4 concentration is a contributing variable, it is not a direct proxy for CH_4 fluxes, which is the covariate of interest for greenhouse gas inventories (Crooks et al., 2018), emission reduction goals (Kroeger et al., 2017), and inversion modeling (Nesser et al., 2024). For CH_4 to be emitted, it needs to not only be present in the porewater, but also needs to ascend through soil layers and avoid oxidation (Blair and Aller, 1995; Laanbroek, 2010). The conveyance of porewater CH_4 to atmospheric emissions is primarily facilitated by plant transport, and secondarily by ebullition and lateral exchange with floodwaters (Bubier et al., 1995; Couwenberg et al., 2011; Sutton-Grier and Megonigal 2011; Mueller et al., 2016; Santos et al., 2019; Bansal et al., 2020; Vroom et al., 2022; Bastviken et al., 2023). A recent synthesis of USA coastal wetland CH_4 emissions data reported a poor relationship with porewater CH_4 concentration (Arias-Ortiz et al., 2024). However, this differs from previous studies (Yang et al., 2019; Villa et al., 2020; Capooci et al., 2024). For example, high porewater CH_4 concentrations sampled in one estuarine site at 15.5 cm subsurface strongly correlated to CH_4 emissions captured at the surface (Capooci et al., 2024). The lack of a clear relationship between CH_4 emissions and porewater CH_4 concentrations likely reflects the complex interaction of production, consumption, and transport activities that control porewater CH_4 inventories across multiple spatial scales.

One potential tool for disentangling the roles of methane production, consumption and transport, as well as porewater and flux data, is the Peatland Ecosystem Photosynthesis Respiration and Methane Transport (PEPRMT) model. In PEPRMT, porewater CH_4 is an unobserved state, with CH_4 flux as the output variable (Oikawa et al., 2017). In future studies, our observations of porewater CH_4, as well as CH_4 flux data, could all be integrated into models, like PEPRMT, using a state-space framework (Dietze, 2017). This type of framework can leverage multiple types of observations (concentrations, fluxes) to constrain model behavior, reduce uncertainty, and improve systems-level understanding.

Future work could identify the relevant mechanisms of production and consumption in tidal wetland soils. To accomplish this, it is necessary to understand which types of methanogens and methanotrophs are present. This may be accomplished by incorporating sequencing work, such as 16S rRNA gene sequencing and quantitative PCR assays, both previously used (Schubert et al., 2011; Hu et al., 2014) in wetlands to elucidate the specific species and which substrates or covariates they utilize.

As a final note, the participatory-nature of this study benefited the project by producing a larger sample size that could not have been feasibly collected by a single team and a higher-quality dataset that benefited from local expertise in siting sampling locations. The National Estuarine Research Reserve System (NERRS) proved to be a valuable resource for a national scale survey of tidal wetland biogeochemical conditions. With both personnel and a publicly accessible standardized data collection and reporting platform (e.g. the Centralized Data Management Office, CDMO), the 30-site (as of this writing) NERRS network and data archive enhances research capacity for co-located and upscaled assessments of coastal processes. Coordinating remote training and kit-based sampling may be a viable alternative to travel-based field work which can lower the carbon footprint of science, provide training, networking and inclusion opportunities for junior researchers, as well as benefit the project by integrating the deeper expertise of those working in these locations.

5. Conclusion

This study draws on a unique dataset built from 367 plots sampled

across 27 sites distributed across 19 coastal states, covering climate zones, coastal typologies (river-, tide-, or wave-dominated), salinity gradients (fresh to brine: 0.5–55 psu), and dominant coastal marsh vegetation communities (109 plant species) in the USA. This work clarifies cross-site and regional trends in porewater CH_4 and its environmental correlates, which was not attainable from previous site-specific studies. We found several key results that provided support for the majority of our hypotheses.

Our first hypothesis that porewater CH_4 decreased with increases in SO_4^{2-} was supported. Particularly, the broad geographic coverage of our data revealed a novel breakpoint in the relationship between porewater SO_4^{2-} and CH_4 when SO_4^{2-} is 0.62 mM. This breakpoint presumably reflects the concentration at, and below which SO_4^{2-} reduction rates start to become limited by SO_4^{2-} availability, and competition for electron donors between methanogens and SO_4^{2-} reducers begins to weaken. Our second hypothesis that salinity is a proxy for SO_4^{2-} predicting porewater CH_4 concentrations was supported. While salinity is significantly correlated with CH_4 because it is strongly intercorrelated with SO_4^{2-}, it is not an ideal proxy for porewater CH_4 concentration due to decoupling of the salinity and SO_4^{2-} relationship, especially for the freshwater tidal wetlands. Our third hypothesis was partially supported, where SO_4^{2-} explained most of the variability in porewater CH_4 relative to variables investigated (salinity, NH_4^+, total Fe, and Z^*_{MHW}). Residual variation in the CH_4-SO_4^{2-} relationship was partially explained by porewater NH_4^+, with no additional variation explained by total Fe or Z^*_{MHW}. This finding suggests that porewater NH_4^+ concentration may also be useful for scaling CH_4 emissions using a threshold of 44 μM CH_4, but the mechanisms behind the threshold are presently unclear and deserve additional research. Additionally, our results show that porewater CH_4 was increasingly variable at relatively wider spatial scales, suggesting that differences among sites may be partly explained by distinct dominant coastal typologies and climate zones. Considering that the dominant sources of variation in porewater CH_4 were within and between site differences, these results suggest that moderate spatial resolution remote sensing products (e.g., 10 × 10 to 30 × 30 m) are appropriate for constraining variation along the most important spatial gradients that control porewater CH_4 concentrations.

Importantly, while this study delivers the first national-scale survey of tidal marsh porewater CH_4 concentrations and commonly-measured biogeochemical covariates, future work is needed to determine whether CH_4 fluxes follow the same spatial patterns of porewater CH_4 concentration considering that net CH_4 emissions are controlled simultaneously by production, consumption, and transport, all of which vary with soil depth and time. However, additional studies and carbon inventories could use this continental-scale dataset to inform sampling strategies that optimize generation of new data relative to the cost of deploying and maintaining monitoring infrastructure. On that note, our field survey approach – highly collaborative, with a low-cost and low-latency field collection and lab analysis protocols – provides a successful template to advance carbon monitoring in coastal wetlands across spatial and temporal scales.

CRediT authorship contribution statement

Erika L. Koontz: Investigation, study design, project administration, writing- original draft preparation, review & editing. **Sarah M. Parker:** Data curation, investigation, visualization, writing- review & editing. **Alice E. Stearns:** Investigation, writing- review & editing. **Brian J. Roberts:** Funding acquisition, study design, investigation, writing- review & editing. **Caitlin M. Young:** Investigation, writing- review & editing. **Lisamarie Windham-Myers:** Funding acquisition, writing- review & editing. **Patricia Y. Oikawa:** Funding acquisition, writing- review & editing. **J. Patrick Megonigal:** Funding acquisition, study design, writing- review & editing. **Genevieve L. Noyce:** Study design, writing- review & editing. **Edward J. Buskey, R. Kyle Derby, Robert P. Dunn, Matthew C. Ferner, Julie L. Krask, Christina M. Marconi, Kelley B. Savage, Julie Shahan, Amanda C. Spivak, Kari A. St. Laurent, Jacob M. Argueta, Steven J. Baird, Kathryn M. Beheshti, Laura C. Crane, Kimberly A. Cressman, Jeffrey A. Crooks, Sarah H. Fernald, Jason A. Garwood, Jason S. Goldstein, Thomas M. Grothues, Andrea Habeck, Scott B. Lerberg, Samantha B. Lucas, Pamela Marcum, Christopher R. Peter, Scott W. Phipps, Kenneth B. Raposa, Andre S. Rovai, Shon S. Schooler, Robert R. Twilley, Megan C. Tyrrell, Kellie A. Uyeda, Sophie H. Wulfing, Jacob T. Aman, Amanda Giacchetti, and Shelby N. Cross-Johnson:** Investigation, writing- review & editing. **James R. Holmquist:** Conceptualization, study design, investigation, formal analysis, funding acquisition, visualization, writing- original draft preparation, review & editing.

Declaration of competing interest

Erika L. Koontz, James R. Holmquist reports financial support was provided by NASA. Sarah M. Parker, Alice E. Stearns, Brian J. Roberts, Patricia Y. Oikawa, J. Patrick Megonigal reports financial support was provided by NASA. J. Patrick Megonigal, Amanda C. Spivak reports was provided by National Science Foundation. James R. Holmquist reports was provided by US Department of Energy. Andre S. Rovai, Robert R. Twilley reports was provided by US Army Engineer Research and Development Center. Amanda C. Spivak reports was provided by US Coastal Research Program. If there are other authors, they declare that they have no known competing financial interests or personal relationships that could have appeared to influence the work reported in this paper.

Acknowledgements

Author E.L.K. thanks J.R.H. for his invaluable mentorship and the opportunity to lead this work. E.L.K and J.R.H would like to express their sincere thanks to the NERRS and associated co-authors for their sampling efforts. We express our deepest gratitude and appreciation for our colleague Lisamarie Windham-Myers (affiliated with the United States Geological Survey and the California Delta Stewardship Council) who was instrumental in the acquisition of funding for the study and editing and review of the manuscript drafts. Additionally, we thank the following individuals for general assistance in the field to support data collection: Stephen Brown, Jaquita Crawford, Nikki Dix, Margaret Dolan, Robin Echols-Booth, Conrad Field, Chris Guo, Karis Kang, Alee Knoell, Jessica Lyins, Casey McClure, Grant Mcknown, Jon Mitchell, Griffin Pinkus, Christopher Ring, Miranda Rosen, James Schloemer, Jake Stocki, Laurel Sullivan, Jordan-destinee Tarleton, Margaret Tomyako, and Catherine Wessell. We thank Jaxine Wolfe and Aaron Carr for their assistance with the data publication. We also thank three anonymous reviewers for their detailed suggestions that greatly improved the manuscript. This study was funded by a grant awarded from the National Aeronautics and Space Administration Carbon Monitoring System (NASA-CMS 80NSSC20K0084). Support was provided by the Smithsonian Environmental Research Center, the National Science Foundation Long-Term Research in Environmental Biology Program (DEB-0950080, DEB-1457100, DEB-1557009, DEB-2051343), the US Department of Energy, Office of Science, Office of Biological and Environmental Research, Environmental System Science program through the COMPASS-FME project (DE-AC05-76RL01830) and awards under the Federal Coastal Zone Management Act, administered by the National Oceanic and Atmospheric Administration's Office for Coastal Management to the participating National Estuarine Research Reserves. A.S.R. and R.R.T. participation was supported by the ACTIONS project with the U.S. Army Engineering, Research and Development Center (W912HZ2020070). A.C.S. participated with support from the US Coastal Research Program (W912HZ-20-2-0053) and the Georgia Coastal Ecosystems Long-Term Ecological Research Project (NSF OCE 1832178). Any use of trade, firm, or product names is for descriptive purposes only and does not imply endorsement by the U.S. Government.

Appendix A. Supplementary data

Supplementary data to this article can be found online at https://doi.org/10.1016/j.scitotenv.2024.177290.

Data availability

Dataset: Porewater covariates from coastal tidal wetlands in the United States (Original data) (Figshare)

References

Adam, Elhadi, Mutanga, Onisimo, Rugege, Denis, 2010. Multispectral and hyperspectral remote sensing for identification and mapping of wetland vegetation: a review. Wetl. Ecol. Manag. 18 (3), 281–296. https://doi.org/10.1007/s11273-009-9169-z.

Al-Haj, A.N., Fulweiler, R.W., 2020. A synthesis of methane emissions from shallow vegetated coastal ecosystems. Glob. Chang. Biol. 26 (5), 2988–3005. https://doi.org/10.1111/gcb.15046.

Arias-Ortiz, A., Wolfe, J., Bridgham, S.D., Knox, S., McNicol, G., Needelman, B.A., Shahan, J., Stuart-Haëntjens, E.J., Windham-Myers, L., Oikawa, P.Y., Baldocchi, D. D., Caplan, J.S., Capooci, M., Czapla, K.M., Derby, R.K., Diefenderfer, H.L., Forbrich, I., Groseclose, G., Keller, J.K., Kelley, C., Keshta, A.E., Kleiner, H.S., Krauss, K.W., Lane, R.R., Mack, S., Moseman-Valtierra, S., Mozdzer, T.J., Mueller, P., Neubauer, S.C., Noyce, G., Schäfer, K.V., Sanders-DeMott, R., Schutte, C.A., Vargas, R., Weston, N.B., Wilson, B., Megonigal, J.P., Holmquist, J.R., 2024. Methane fluxes in tidal marshes of the conterminous United States. Glob. Chang. Biol. 30 (9). https://doi.org/10.1111/gcb.17462.

Arias-Ortiz, Ariane, Oikawa, Patricia Y., Carlin, Joseph, Masqué, Pere, Shahan, Julie, Kanneg, Sadie, Paytan, Adina, Baldocchi, Dennis D., 2021. Tidal and nontidal marsh restoration: a trade-off between carbon sequestration, methane emissions, and soil accretion. J. Geophys. Res. Biogeosci. 126 (12). https://doi.org/10.1029/2021jg006573.

Bansal, Sheel, Johnson, Olivia F., Meier, Jacob, Zhu, Xiaoyan, 2020. Vegetation affects timing and location of wetland methane emissions. J. Geophys. Res. Biogeosci. 125 (9). https://doi.org/10.1029/2020JG005777.

Bao, T., Jia, G., Xu, X., 2021. Wetland heterogeneity determines methane emissions: a pan-Arctic synthesis. Environ. Sci. Technol. 55 (14), 10152–10163. https://doi.org/10.1021/acs.est.1c01616.

Bartlett, Karen B., Bartlett, David S., Harriss, Robert C., Sebacher, Daniel I., 1987. Methane emissions along a salt marsh salinity gradient. Biogeochemistry 4. https://doi.org/10.1007/BF02187365.

Bastviken, David, Treat, Claire C., Pangala, Sunitha Rao, Gauci, Vincent, Enrich-Prast, Alex, Karlson, Martin, Gålfalk, Magnus, Romano, Mariana Brandini, Sawakuchi, Henrique Oliveira, 2023. The importance of plants for methane emission at the ecosystem scale. Aquat. Bot. 184. https://doi.org/10.1016/j.aquabot.2022.103596.

Beck, H.E., Zimmermann, N.E., McVicar, T.R., Vergopolan, N., Berg, A., Wood, E.F., 2018. Present and future Köppen-Geiger climate classification maps at 1-km resolution. Sci. Data 5 (1), 180214. https://doi.org/10.1038/sdata.2018.214.

Bell, S., Cornford, D., Bastin, L., 2013. The state of automated amateur weather observations. Weather 68 (2), 36–41. https://doi.org/10.1002/wea.1980.

Blair, N.E., Aller, R.C., 1995. Anaerobic methane oxidation on the Amazon shelf. Geochim. Cosmochim. Acta 59 (18), 3707–3715. https://doi.org/10.1016/0016-7037(95)00277-7.

Bowen, Jennifer L., Giblin, Anne E., Murphy, Anna E., Bulseco, Ashley N., Deegan, Linda A., Johnson, David S., Nelson, James A., Mozdzer, Thomas J., Sullivan, Hillary L., 2020. Not all nitrogen is created equal: differential effects of nitrate and ammonium enrichment in coastal wetlands. BioScience 70 (12), 1108–1119. https://doi.org/10.1093/biosci/biaa140.

Braun-Blanquet, Josias, 1932. Plant Sociology. The Study of Plant Communities. McGraw-Hill Book Co., Inc., New York and London.

Bridgham, S.D., Megonigal, J.P., Keller, J.K., Bliss, N.B., Trettin, C., 2006. The carbon balance of North American wetlands. Wetlands 26 (4), 889–916. https://doi.org/10.1672/0277-5212(2006)26[889:TCBONA]2.0.CO;2.

Brown, Molly E., Mitchell, Catherine, Halabisky, Meghan, Gustafson, Benjamin, do Rosario Gomes, Helga, Goes, Joaquim I., Zhang, Xuesong, Campbell, Anthony D., Poulter, Benjamin, 2023. Assessment of the NASA carbon monitoring system wet carbon stakeholder community: data needs, gaps, and opportunities. Environ. Res. Lett. 18 (8), 084005. https://doi.org/10.1088/1748-9326/ace208.

Bubier, Jill L., Moore, Tim R., Bellisario, Lianne, Comer, Neil T., Crill, Patrick M., 1995. Ecological controls on methane emissions from a northern peatland complex in the zone of discontinuous permafrost, Manitoba, Canada. Glob. Biogeochem. Cycles 9 (4), 455–470. https://doi.org/10.1029/95GB02379.

Capooci, Margaret, Seyfferth, Angelia L., Tobias, Craig, Wozniak, Andrew S., Hedgpeth, Alexandra, Bowen, Malique, Biddle, Jennifer F., McFarlane, Karis J., Vargas, Rodrigo, 2024. High methane concentrations in tidal salt marsh soils: where does the methane go? Glob. Chang. Biol. 30 (1), e17050. https://doi.org/10.1111/gcb.17050.

Cassaway, A.F., Twilley, R.R., Rovai, A.S., Snedden, G.A., 2024. Patterns of marsh surface accretion rates along salinity and hydroperiod gradients between active and inactive coastal deltaic floodplains. Estuar. Coast. Shelf Sci. 301 (108757), 108757. https://doi.org/10.1016/j.ecss.2024.108757.

Chambers, L.G., Osborne, T.Z., Reddy, K.R., 2013. Effect of salinity-altering pulsing events on soil organic carbon loss along an intertidal wetland gradient: a laboratory experiment. Biogeochemistry 115 (1–3), 363–383. https://doi.org/10.1007/s10533-013-9841-5.

Chen, Meilian, Lee, Jong Hyeon, Hur, Jin, 2015. Effects of sampling methods on the quantity and quality of dissolved organic matter in sediment pore waters as revealed by absorption and fluorescence spectroscopy. Environ. Sci. Pollut. Res. 22 (19), 14841–14851. https://doi.org/10.1007/s11356-015-4656-7.

Chmura, Gail L., Anisfeld, Shimon C., Cahoon, Donald R., Lynch, James C., 2003. Global carbon sequestration in tidal, saline wetland soils. Glob. Biogeochem. Cycles 17 (4), 1111. https://doi.org/10.1029/2002GB001917.

Chowdhury, Taniya Roy, Dick, Richard P., 2013. Ecology of aerobic methanotrophs in controlling methane fluxes from wetlands. Appl. Soil Ecol. Sect. Agric. Ecosyst. Environ. 65 (March), 8–22. https://doi.org/10.1016/j.apsoil.2012.12.014.

Corstanje, R., Kirk, G.J.D., Lark, R.M., 2008a. The behaviour of soil process models of ammonia volatilization at contrasting spatial scales. Eur. J. Soil Sci. 59 (6), 1271–1283. https://doi.org/10.1111/j.1365-2389.2008.01086.x.

Corstanje, R., Kirk, G.J.D., Pawlett, M., Read, R., Lark, R.M., 2008b. Spatial variation of ammonia volatilization from soil and its scale-dependent correlation with soil properties. Eur. J. Soil Sci. 59 (6), 1260–1270. https://doi.org/10.1111/j.1365-2389.2008.01087.x.

Cotovicz Jr., L.C., Abril, G., Sanders, C.J., Tait, D.R., Maher, D.T., Sippo, J.Z., Holloway, C., Yau, Y.Y.Y., Santos, I.R., 2024. Methane oxidation minimizes emissions and offsets to carbon burial in mangroves. Nat. Clim. Chang. 14 (3), 275–281. https://doi.org/10.1038/s41558-024-01927-1.

Couwenberg, John, Thiele, Annett, Tanneberger, Franziska, Augustin, Jürgen, Bärisch, Susanne, Dubovik, Dimitry, Liashchynskaya, Nadzeya, et al., 2011. Assessing greenhouse gas emissions from peatlands using vegetation as a proxy. Hydrobiologia 674 (1), 67–89. https://doi.org/10.1007/s10750-011-0729-x.

Crawford, T.W., 2009. Scale analytical. In: International Encyclopedia of Human Geography, pp. 26–39. https://doi.org/10.1016/B978-008044910-4.00399-0.

Crooks, S., Sutton-Grier, A.E., Troxler, T.G., Herold, N., Bernal, B., Schile-Beers, L., Wirth, T., 2018. Coastal wetland management as a contribution to the US National Greenhouse Gas Inventory. Nat. Clim. Chang. 8 (12), 1109–1112. https://doi.org/10.1038/s41558-018-0345-0.

Derby, R. Kyle, Needelman, Brian A., Roden, Ana A., Megonigal, J.P., 2022. Vegetation and hydrology stratification as proxies to estimate methane emission from tidal marshes. Biogeochemistry 157 (2), 227–243. https://doi.org/10.1007/s10533-021-00870-z.

Dietze, Michael, 2017. Ecological Forecasting. Princeton University Press, Princeton. https://doi.org/10.1515/9781400885459.

Duan, H., Xiao, Q., Qi, T., Hu, C., Zhang, M., Shen, M., Hu, Z., Wang, W., Xiao, W., Qiu, Y., Luo, J., Lee, X., 2023. Quantification of diffusive methane emissions from a large eutrophic lake with satellite imagery. Environ. Sci. Technol. 57 (36), 13520–13529. https://doi.org/10.1021/acs.est.3c05631.

Dürr, H.H., Laruelle, G.G., van Kempen, C.M., Slomp, C.P., Meybeck, M., Middelkoop, H., 2011. Worldwide typology of nearshore coastal systems: defining the estuarine filter of river inputs to the oceans. Estuaries Coast 34 (3), 441–458. https://doi.org/10.1007/s12237-011-9381-y.

Environmental Protection Agency, 1996. Method 9030B: acid-soluble and acid-insoluble sulfides: distillation. In: Test Methods for Evaluating Solid Waste, Physical/Chemical Methods, EPA Publication SW-846, 3rd ed. Environmental Protection Agency. 9030B-1-9030B-15. https://www.epa.gov/sites/default/files/2015-12/documents/9030b.pdf.

Environmental Systems Research Institute, Inc, 2020. ArcGIS (Version 10.8).

Fargione, Joseph E., Bassett, Steven, Boucher, Timothy, Bridgham, Scott D., Conant, Richard T., Cook-Patton, Susan C., Ellis, Peter W., et al., 2018. Natural climate solutions for the United States. Sci. Adv. 4 (11), eaat1869. https://doi.org/10.1126/sciadv.aat1869.

Faust, D.R., Liebig, M.A., 2018. Effects of storage time and temperature on greenhouse gas samples in Exetainer vials with chlorobutyl septa caps. MethodsX 5, 857–864. https://doi.org/10.1016/j.mex.2018.06.016.

Guo, Meng, Li, Jing, Sheng, Chunlei, Jiawei, Xu, Li, Wu., 2017. A review of wetland remote sensing. Sensors 17 (4). https://doi.org/10.3390/s17040777.

Hadj-Hammou, J., Loiselle, S., Ophof, D., Thornhill, I., 2017. Getting the full picture: assessing the complementarity of citizen science and agency monitoring data. PLoS One 12 (12), e0188507. https://doi.org/10.1371/journal.pone.0188507.

Helton, A.M., Bernhardt, E.S., Fedders, A., 2014. Biogeochemical regime shifts in coastal landscapes: the contrasting effects of saltwater incursion and agricultural pollution on greenhouse gas emissions from a freshwater wetland. Biogeochemistry 120 (1–3), 133–147. https://doi.org/10.1007/s10533-014-9986-x.

Hinrichs, K.-U., Boetius, A., 2002. The anaerobic oxidation of methane: new insights in microbial ecology and biogeochemistry. In: Ocean Margin Systems. Springer Berlin Heidelberg, pp. 457–477. https://doi.org/10.1007/978-3-662-05127-6_28.

Hobbs, N. Thompson, Hooten, Mevin B., 2015. Bayesian Models. Princeton University Press. https://doi.org/10.1515/9781400866557.

Holmer, Marianne, Storkholm, Peter, 2001. Sulphate reduction and sulphur cycling in lake sediments: a review. Freshw. Biol. 46 (4), 431–451. https://doi.org/10.1046/j.1365-2427.2001.00687.x.

Holmquist, James R., Windham-Myers, Lisamarie, 2022. A conterminous USA-scale map of relative tidal marsh elevation. Estuar. Coasts. https://doi.org/10.1007/s12237-021-01027-9.

Holmquist, James R., Windham-Myers, Lisamarie, Bernal, Blanca, Byrd, Kristin B., Crooks, Steve, Gonneea, Meagan Eagle, Herold, Nate, et al., 2018. Uncertainty in

United States coastal wetland greenhouse gas inventorying. Environ. Res. Lett. 13 (11). https://doi.org/10.1088/1748-9326/aae157.

Hu, B.-L., Shen, L.-D., Lian, X., Zhu, Q., Liu, S., Huang, Q., He, Z.-F., Geng, S., Cheng, D.-Q., Lou, L.-P., Xu, X.-Y., Zheng, P., He, Y.-F., 2014. Evidence for nitrite-dependent anaerobic methane oxidation as a previously overlooked microbial methane sink in wetlands. Proc. Natl. Acad. Sci. USA 111 (12), 4495–4500. https://doi.org/10.1073/pnas.1318393111.

Huang, Chang, Chen, Yun, Zhang, Shiqiang, Jianping, Wu., 2018. Detecting, extracting, and monitoring surface water from space using optical sensors: a review. Rev. Geophys. 56 (2), 333–360. https://doi.org/10.1029/2018RG000598.

Hurtt, George C., Andrews, Arlyn, Bowman, Kevin, Brown, Molly E., Chatterjee, Abhishek, Escobar, Vanessa, Fatoyinbo, Lola, et al., 2022. The NASA carbon monitoring system phase 2 synthesis: scope, findings, gaps and recommended next steps. Environ. Res. Lett. 17 (6), 063010. https://doi.org/10.1088/1748-9326/ac7407.

Ingvorsen, K., Zehnder, A.J., Jørgensen, B.B., 1984. Kinetics of sulfate and acetate uptake by *Desulfobacter postgatei*. Appl. Environ. Microbiol. 47 (2), 4038. https://doi.org/10.1128/aem.47.2.403-408.1984.

Johnson, R.K., Furse, M.T., Hering, D., Sandin, L., 2007. Ecological relationships between stream communities and spatial scale: implications for designing catchment-level monitoring programmes. Freshw. Biol. 52 (5), 939–958. https://doi.org/10.1111/j.1365-2427.2006.01692.x.

Keiluweit, M., Gee, K., Denney, A., Fendorf, S., 2018. Anoxic microsites in upland soils dominantly controlled by clay content. Soil Biol. Biochem. 118, 42–50. https://doi.org/10.1016/j.soilbio.2017.12.002.

Keller, Jason K., Wolf, Amelia A., Weisenhorn, Pamela B., Drake, Bert G., Patrick Megonigal, J., 2009. Elevated CO_2 affects porewater chemistry in a brackish marsh. Biogeochemistry 96 (1), 101–117. https://doi.org/10.1007/s10533-009-9347-3.

Kirwan, M.L., Megonigal, J.P., Noyce, G.L., Smith, A.J., 2023. Geomorphic and ecological constraints on the coastal carbon sink. Nat. Rev. Earth Environ. 4 (6), 393–406. https://doi.org/10.1038/s43017-023-00429-6.

Koontz, Erika L., Parker, Sarah M., Stearns, Alice E., Roberts, Brian J., Young, Caitlin M., Windham-Myers, Lisamarie, Oikawa, Patricia Y., Megonigal, Patrick J., Noyce, Genevieve L., Buskey, Edward J., Derby, Kyle R., Dunn, Robert P., Ferner, Matthew C., Krask, Julie L., Marconi, Christina M., Savage, Kelley B., Shahan, Julie, Spivak, Amanda C., St. Laurent, Kari, Argueta, Jacob M., Baird, Steven J., Beheshti, Kathryn M., Crane, Laura C., Cressman, Kimberly A., Crooks, Jeffrey A., Fernald, Sarah H., Garwood, Jason A., Goldstein, Jason S., Grothues, Thomas M., Habeck, Andrea, Lerberg, Scott B., Lucas, Samantha B., Marcum, Pamela, Peter, Christopher R., Phipps, Scott W., Raposa, Kenneth B., Rovai, Andre S., Schooler, Shon S., Twilley, Robert R., Tyrrell, Megan C., Uyeda, Kellie A., Wulfing, Sophie H., Aman, Jacob T., Giacchetti, Amanda, Cross-Johnson, Shelby N., Holmquist, James R., 2024. Dataset: porewater covariates from coastal tidal wetlands in the United States [data set]. In: Controls on Spatial Variation in Porewater Methane Concentrations Across United States Tidal Wetlands. https://doi.org/10.25573/serc.25152206. https://smithsonian.figshare.com/articles/dataset/Dataset_Porewater_covariates_from_coastal_tidal_wetlands_in_the_United_States/25152206.

Krask, Julie L., Buck, Tracy L., Dunn, Robert P., Smith, Erik M., 2022. Increasing tidal inundation corresponds to rising porewater nutrient concentrations in a southeastern U.S. salt marsh. PLoS One 17 (11), e0278215. https://doi.org/10.1371/journal.pone.0278215.

Kristjansson, J.K., Schönheit, P., 1983. Why do sulfate-reducing bacteria outcompete methanogenic bacteria for substrates? Oecologia 60 (2), 264–266. https://doi.org/10.1007/bf00379530.

Kroeger, Kevin D., Crooks, Stephen, Moseman-Valtierra, Serena, Tang, Jianwu, 2017. Restoring tides to reduce methane emissions in impounded wetlands: a new and potent blue carbon climate change intervention. Sci. Rep. 7 (1), 11914. https://doi.org/10.1038/s41598-017-12138-4.

Kuivila, K.M., Murray, J.W., Devol, A.H., 1989. Methane production, sulfate reduction and competition for substrates in the sediments of Lake Washington. Geochim. Cosmochim. Acta 53, 409–416. https://doi.org/10.1016/0016-7037(89)90392-X.

Laanbroek, Hendrikus J., 2010. Methane emission from natural wetlands: interplay between emergent macrophytes and soil microbial processes. A mini-review. Ann. Bot. 105 (1), 141–153. https://doi.org/10.1093/aob/mcp201.

Langley, A.J., Mozdzer, T.J., Shepard, K.A., Hagerty, S.B., Megonigal, J.P., 2013. Tidal marsh plant responses to elevated CO_2, nitrogen fertilization, and sea level rise. Glob. Chang. Biol. 19 (5), 1495–1503. https://doi.org/10.1111/gcb.12147.

Li, M., Kort, E.A., Bloom, A.A., Wu, D., Plant, G., Gerlein-Safdi, C., Pu, T., 2024. Underestimated dry season methane emissions from wetlands in the Pantanal. Environ. Sci. Technol. https://doi.org/10.1021/acs.est.3c09250.

Loeppert, Richard H., Inskeep, William P., 1996. Chapter 23 Iron. In: Sparks, D.L., Page, A.L., Helmke, P.A., Loeppert, R.H., Soltanpour, P.N., Tabatabai, M.A., Johnston, C.T., Sumner, M.E. (Eds.), Methods of Soils Analysis, Part 3: Chemical Methods, 1st ed. Soil Science Society of America, Inc. and the American Society of Agronomy, Inc., pp. 639–664. https://doi.org/10.2136/sssabookser5.3

Lovley, Derek R., Klug, Michael J., 1983. Sulfate reducers can outcompete methanogens at freshwater sulfate concentrations. Appl. Environ. Microbiol. 45 (1), 187–192. https://doi.org/10.1128/aem.45.1.187-192.1983.

Määttä, T., Malhotra, A., 2024. The hidden roots of wetland methane emissions. Glob. Chang. Biol. 30 (2), e17127. https://doi.org/10.1111/gcb.17127.

Mcleod, E., Chmura, G.L., Bouillon, S., Salm, R., Björk, M., Duarte, C.M., Lovelock, C.E., Schlesinger, W.H., Silliman, B.R., 2011. A blueprint for blue carbon: toward an improved understanding of the role of vegetated coastal habitats in sequestering CO_2. Front. Ecol. Environ. 9 (10), 552–560. https://doi.org/10.1890/110004.

Megonigal, J.P., Schlesinger, W.H., 2002. Methane-limited methanotrophy in tidal freshwater swamps. Glob. Biogeochem. Cycles. https://doi.org/10.1029/2001GB001594.

Megonigal, J.P., Mines, M.E., Visscher, P.T., 2004. Anaerobic metabolism: linkages to trace gases and aerobic processes. In: Biogeochemistry, pp. 317–413. https://repository.si.edu/bitstream/handle/10088/15579/Megonigal_Hines_Visscher_2004.pdf.

Mountfort, D.O., Asher, R.A., Mays, E.L., Tiedje, J.M., 1980. Carbon and electron flow in mud and sandflat intertidal sediments at Delaware Inlet, Nelson, New Zealand. Appl. Environ. Microbiol. 39 (4), 686–694. https://doi.org/10.1128/aem.39.4.686-694.1980.

Mueller, Peter, Jensen, Kai, Megonigal, James Patrick, 2016. Plants mediate soil organic matter decomposition in response to sea level rise. Glob. Chang. Biol. 22 (1), 404–414. https://doi.org/10.1111/gcb.13082.

Muggeo, Vito M.R., 2008. segmented: An R Package to Fit Regression Models with Broken-Line Relationships. R News. May 2008. https://journal.r-project.org/articles/RN-2008-004/RN-2008-004.pdf.

Murphy, Rebecca R., Curriero, Frank C., Ball, William P., 2010. Comparison of spatial interpolation methods for water quality evaluation in the Chesapeake Bay. J. Environ. Eng. 136 (2), 160–171. https://doi.org/10.1061/(ASCE)EE.1943-7870.0000121.

Needelman, Brian A., Emmer, Igino M., Emmett-Mattox, Stephen, Stephen Crooks, J., Megonigal, Patrick, Myers, Doug, Oreska, Matthew P.J., McGlathery, Karen, 2018. The science and policy of the verified carbon standard methodology for tidal wetland and seagrass restoration. Estuaries Coast 41 (8), 2159–2171. https://doi.org/10.1007/s12237-018-0429-0.

Nesser, H., Jacob, D.J., Maasakkers, J.D., Lorente, A., Chen, Z., Lu, X., Randles, C., 2024. High-resolution US methane emissions inferred from an inversion of 2019 TROPOMI satellite data: contributions from individual states, urban areas, and landfills. Atmos. Chem. Phys. 24 (8), 5069–5091. https://acp.copernicus.org/articles/24/5069/2024/.

Neubauer, S.C., 2013. Ecosystem responses of a tidal freshwater marsh experiencing saltwater intrusion and altered hydrology. Estuar. Coasts 36 (3), 491–507. https://doi.org/10.1007/s12237-011-9455-x.

Neubauer, Scott C., Megonigal, J.P., 2015. Moving beyond global warming potentials to quantify the climatic role of ecosystems. Ecosystems 18 (6), 1000–1013. https://doi.org/10.1007/s10021-015-9879-4.

Noyce, Genevieve L., Megonigal, J.P., 2021. Biogeochemical and plant trait mechanisms drive enhanced methane emissions in response to whole-ecosystem warming. Biogeosciences 18 (8), 2449–2463. https://doi.org/10.5194/bg-18-2449-2021.

Noyce, Genevieve L., Kirwan, Matthew L., Rich, Roy L., Megonigal, J.P., 2019. Asynchronous nitrogen supply and demand produce nonlinear Plant allocation responses to warming and elevated CO_2. Proc. Natl. Acad. Sci. USA 116 (43), 21623–21628. https://doi.org/10.1073/pnas.1904990116.

Oikawa, P.Y., Jenerette, G.D., Knox, S.H., Sturtevant, C., Verfaillie, J., Dronova, I., Poindexter, C.M., Eichelmann, E., Baldocchi, D.D., 2017. Evaluation of a hierarchy of models reveals importance of substrate limitation for predicting carbon dioxide and methane exchange in restored wetlands. J. Geophys. Res. Biogeosci. 122 (January), 145–167. https://doi.org/10.1002/2016JG003438.

Pardo, L.H., Fenn, M.E., Goodale, C.L., Geiser, L.H., Driscoll, C.T., Allen, E.B., Baron, J.S., Bobbink, R., Bowman, W.D., Clark, C.M., Emmett, B., Gilliam, F.S., Greaver, T.L., Hall, S.J., Lilleskov, E.A., Liu, L., Lynch, J.A., Nadelhoffer, K.J., Perakis, S.S., et al., 2011. Effects of nitrogen deposition and empirical nitrogen critical loads for ecoregions of the United States. Ecol. Appl. 21 (8), 3049–3082. https://doi.org/10.1890/10-2341.1.

Pendleton, L., Donato, D.C., Murray, B.C., Crooks, S., Jenkins, W.A., Sifleet, S., Craft, C., Fourqurean, J.W., Kauffman, J.B., Marbà, N., Megonigal, P., Pidgeon, E., Herr, D., Gordon, D., Baldera, A., 2012. Estimating global "blue carbon" emissions from conversion and degradation of vegetated coastal ecosystems. PLoS One 7 (9), e43542. https://doi.org/10.1371/journal.pone.0043542.

Perez-Coronel, E., Beman, J.M., 2022. Multiple sources of aerobic methane production in aquatic ecosystems include bacterial photosynthesis. Nat. Commun. 13, 6454. https://doi.org/10.1038/s41467-022-34105-y.

Perryman, C.R., McCalley, C.K., Ernakovich, J.G., Lamit, L.J., Shorter, J.H., Lilleskov, E., Varner, R.K., 2022. Microtopography matters: belowground CH $_4$ cycling regulated by differing microbial processes in peatland hummocks and lawns. J. Geophys. Res. Biogeosci. 127 (8). https://doi.org/10.1029/2022jg006948.

Plummer, Martyn, Stukalov, Alexey, Denwood, Matt, 2021. Rjags: Bayesian graphical models using MCMC (version 4-12). R. https://cran.r-project.org/web/packages/rjags/index.html.

Poffenbarger, Hanna J., Needelman, Brian A., Megonigal, J.P., 2011. Salinity influence on methane emissions from tidal marshes. Wetlands 31 (5), 831–842. https://doi.org/10.1007/s13157-011-0197-0.

R Core Team, 2022. R: A Language and Environment for Statistical Computing. Vienna, Austria. https://www.R-project.org/.

Rosentreter, Judith A., Laruelle, Goulven G., Bange, Hermann W., Bianchi, Thomas S., Busecke, Julius J.M., Cai, Wei-Jun, Eyre, Bradley D., et al., 2023. Coastal vegetation and estuaries are collectively a greenhouse gas sink. Nat. Clim. Chang. 13 (6), 579–587. https://doi.org/10.1038/s41558-023-01682-9.

Santos, Isaac R., Maher, Damien T., Larkin, Reece, Webb, Jackie R., Sanders, Christian J., 2019. Carbon outwelling and outgassing vs. burial in an estuarine tidal creek surrounded by mangrove and saltmarsh wetlands. Limnol. Oceanogr. 64 (3), 996–1013. https://doi.org/10.1002/lno.11090.

Schubert, C.J., Vazquez, F., Lösekann-Behrens, T., Knittel, K., Tonolla, M., Boetius, A., 2011. Evidence for anaerobic oxidation of methane in sediments of a freshwater system (Lago di Cadagno): anaerobic methane oxidation in freshwater sediments.

FEMS Microbiol. Ecol. 76 (1), 26–38. https://doi.org/10.1111/j.1574-6941.2010.01036.x.
Seeberg-Elverfeldt, Jens, Schlüter, Michael, Feseker, Tomas, Kölling, Martin, 2005. Rhizon sampling of porewaters near the sediment-water interface of aquatic systems. Limnol. Oceanogr. Methods/ASLO 3 (8), 361–371. https://doi.org/10.4319/lom.2005.3.361.
Segarra, K.E.A., Comerford, C., Slaughter, J., Joye, S.B., 2013. Impact of electron acceptor availability on the anaerobic oxidation of methane in coastal freshwater and brackish wetland sediments. Geochim. Cosmochim. Acta 115, 15–30. https://doi.org/10.1016/j.gca.2013.03.029.
Segarra, K.E.A., Schubotz, F., Samarkin, V., Yoshinaga, M.Y., Hinrichs, K.-U., Joye, S.B., 2015. High rates of anaerobic methane oxidation in freshwater wetlands reduce potential atmospheric methane emissions. Nat. Commun. 6 (1), 7477. https://doi.org/10.1038/ncomms8477.
Seyfferth, A.L., Bothfeld, F., Vargas, R., Stuckey, J.W., Wang, J., Kearns, K., Michael, H. A., Guimond, J., Yu, X., Sparks, D.L., 2020. Spatial and temporal heterogeneity of geochemical controls on carbon cycling in a tidal salt marsh. Geochim. Cosmochim. Acta 282, 1–18. https://doi.org/10.1016/j.gca.2020.05.013.
Shen, Li-Dong, Liu, Shuai, Zhan-Fei He, Xu, Lian, Qian Huang, He, Yun-Feng, Lou, Li-Ping, Xiang-Yang, Xu, Zheng, Ping, Bao-Lan, Hu., 2015. Depth-specific distribution and importance of nitrite-dependent anaerobic ammonium and methane-oxidising bacteria in an urban wetland. Soil Biol. Biochem. 83 (April), 43–51. https://doi.org/10.1016/j.soilbio.2015.01.010.
Shotbolt, L., 2010. Pore water sampling from lake and estuary sediments using rhizon samplers. J. Paleolimnol. 44 (2), 695–700. https://doi.org/10.1007/s10933-008-9301-8.
Sinke, Anja J.C., Cornelese, Adi A., Cappenberg, Thomas E., Zehnder, Alexander J.B., 1992. Seasonal variation in sulfate reduction and Methanogenesis in peaty sediments of eutrophic Lake Loosdrecht, the Netherlands. Biogeochemistry 16 (1), 43–61. https://doi.org/10.1007/BF02402262.
Sivan, O., Adler, M., Pearson, A., Gelman, F., Bar-Or, I., John, S.G., Eckert, W., 2011. Geochemical evidence for iron-mediated anaerobic oxidation of methane. Limnol. Oceanogr. 56 (4), 1536–1544. https://doi.org/10.4319/lo.2011.56.4.1536.
Song, J., Luo, Y.M., Zhao, Q.G., Christie, P., 2003. Novel use of soil moisture samplers for studies on anaerobic ammonium fluxes across lake sediment-water interfaces. Chemosphere 50 (6), 711–715. https://doi.org/10.1016/S0045-6535(02)00210-2.
Sutton-Grier, Ariana E., Megonigal, J.P., 2011. Plant species traits regulate methane production in freshwater wetland soils. Soil Biol. Biochem. 43 (2), 413–420. https://doi.org/10.1016/j.soilbio.2010.11.009.
Tan, L., Ge, Z., Zhou, X., Li, S., Li, X., Tang, J., 2020. Conversion of coastal wetlands, riparian wetlands, and peatlands increases greenhouse gas emissions: a global meta-analysis. Glob. Chang. Biol. 26 (3), 1638–1653. https://doi.org/10.1111/gcb.14933.
Tobler, W., 2004. On the first law of geography: a reply. Ann. Assoc. Am. Geogr. 94 (2), 304–310. https://doi.org/10.1111/j.1467-8306.2004.09402009.x.
Tobler, W.R., 1970. A computer movie simulating urban growth in the Detroit region. Econ. Geogr. 46, 234. https://doi.org/10.2307/143141.
Tong, Chuan, Wang, Wei-Qi, Zeng, Cong-Sheng, Marrs, Rob, 2010. Methane (CH_4) emission from a tidal marsh in the Min River Estuary, Southeast China. J. Environ. Sci. Health Pt. A Toxic Hazard. Subst. Environ. Eng. 45 (4), 506–516. https://doi.org/10.1080/10934520903542261.
Tong, Chuan, Luo, Min, Huang, Jiafang, She, Chenxin, Li, Yalan, Ren, Peng, 2020. Greenhouse gas fluxes and porewater geochemistry following short-term pulses of saltwater and Fe(III) in a subtropical tidal freshwater estuarine marsh. Geoderma 369 (June). https://doi.org/10.1016/j.geoderma.2020.114340.
Valiela, I., Teal, J.M., 1974. Nutrient limitation in salt marsh vegetation. In: Reimold, R. J., Queen, W.H. (Eds.), Ecology of Halophytes, pp. 547–563 hero.epa.gov. https://doi.org/10.1016/B978-0-12-586450-3.50025-1.
Van Der Nat, F., De Brouwer, J., Middelburg, J.J., Laanbroek, H.J., 1997. Spatial distribution and inhibition by ammonium of methane oxidation in intertidal freshwater marshes. Appl. Environ. Microbiol. 63 (12), 4734–4740. https://doi.org/10.1128/aem.63.12.4734-4740.1997.
Vann, Cheryl D., Megonigal, J.P., 2003. Elevated CO_2 and water depth regulation of methane emissions: comparison of woody and non-woody wetland plant species. Biogeochemistry 63 (2), 117–134. https://doi.org/10.1023/A:1023397032331.
Villa, J.A., Smith, G.J., Ju, Y., Renteria, L., Angle, J.C., Arntzen, E., Harding, S.F., Ren, H., Chen, X., Sawyer, A.H., Graham, E.B., Stegen, J.C., Wrighton, K.C., Bohrer, G., 2020. Methane and nitrous oxide porewater concentrations and surface fluxes of a regulated river. Sci. Total Environ. 715 (136920), 136920. https://doi.org/10.1016/j.scitotenv.2020.136920.
Viollier, E., Inglett, P.W., Hunter, K., Roychoudhury, A.N., Van Cappellen, P., 2000. The Ferrozine Method Revisited: Fe(II)/Fe(III) Determination in Natural Waters. https://doi.org/10.1016/S0883-2927(99)00097-9.
Vroom, R.J.E., van den Berg, M., Pangala, S.R., van der Scheer, O.E., Sorrell, B.K., 2022. Physiological processes affecting methane transport by wetland vegetation — a review. Aquat. Bot. 182 (October). https://doi.org/10.1016/j.aquabot.2022.103547.
Wang, C., Tong, C., Chambers, L.G., Liu, X., 2017. Identifying the salinity thresholds that impact greenhouse gas production in subtropical tidal freshwater marsh soils. Wetlands 37 (3), 559–571. https://doi.org/10.1007/s13157-017-0890-8.
Weston, N.B., Neubauer, S.C., Velinsky, D.J., Vile, M.A., 2014. Net ecosystem carbon exchange and the greenhouse gas balance of tidal marshes along an estuarine salinity gradient. Biogeochemistry 120 (1), 163–189. https://doi.org/10.1007/s10533-014-9989-7.
Weston, Nathaniel B., Porubsky, William P., Samarkin, Vladimir A., Erickson, Matthew, Macavoy, Stephen E., Joye, Samantha B., 2006. Porewater stoichiometry of terminal metabolic products, sulfate, and dissolved organic carbon and nitrogen in estuarine intertidal creek-bank sediments. Biogeochemistry 77 (3), 375–408. https://doi.org/10.1007/s10533-005-1640-1.
Wilson, B.J., Mortazavi, B., Kiene, R.P., 2015. Spatial and temporal variability in carbon dioxide and methane exchange at three coastal marshes along a salinity gradient in a northern Gulf of Mexico estuary. Biogeochemistry 123 (3), 329–347. https://doi.org/10.1007/s10533-015-0085-4.
Winfrey, M.R., Zeikus, J.G., 1977. Effect of sulfate on carbon and electron flow during microbial methanogenesis in freshwater sediments. Appl. Environ. Microbiol. 33 (2), 275–281. https://doi.org/10.1128/aem.33.2.275-281.1977.
Xiao, H., Song, C., Li, S., Lu, X., Liang, M., Xia, X., Yuan, W., 2024. Global wetland methane emissions from 2001 to 2020: magnitude, dynamics and controls. Earth's Future 12 (9). https://doi.org/10.1029/2024ef004794.
Yang, P., Wang, M.H., Lai, D.Y.F., Chun, K.P., Huang, J.F., Wan, S.A., Bastviken, D., Tong, C., 2019. Methane dynamics in an estuarine brackish *Cyperus malaccensis* marsh: production and porewater concentration in soils, and net emissions to the atmosphere over five years. Geoderma 337, 132–142. https://doi.org/10.1016/j.geoderma.2018.09.019.
Zhu, Guibing, Jetten, Mike S.M., Kuschk, Peter, Ettwig, Katharina F., Yin, Chengqing, 2010. Potential roles of anaerobic ammonium and methane oxidation in the nitrogen cycle of wetland ecosystems. Appl. Microbiol. Biotechnol. 86 (4), 1043–1055. https://doi.org/10.1007/s00253-010-2451-4.
Zimmerman, Marc J., Massey, Andrew J., Campo, Kimberly W., 2005. Pushpoint sampling for defining spatial and temporal variations in contaminant concentrations in sediment pore water near the ground-water/surface-water interface. In: Scientific Investigations Report No. 2005-5036. US Department of the Interior, US Geological Survey. https://pubs.usgs.gov/sir/2005/5036/pdf/sir2005_5036.pdf.
Zou, Y., Zhang, S., Huo, L., Sun, G., Lu, X., Jiang, M., Yu, X., 2018. Wetland saturation with introduced Fe(III) reduces total carbon emissions and promotes the sequestration of DOC. Geoderma 325, 141–151. https://doi.org/10.1016/j.geoderma.2018.03.031.